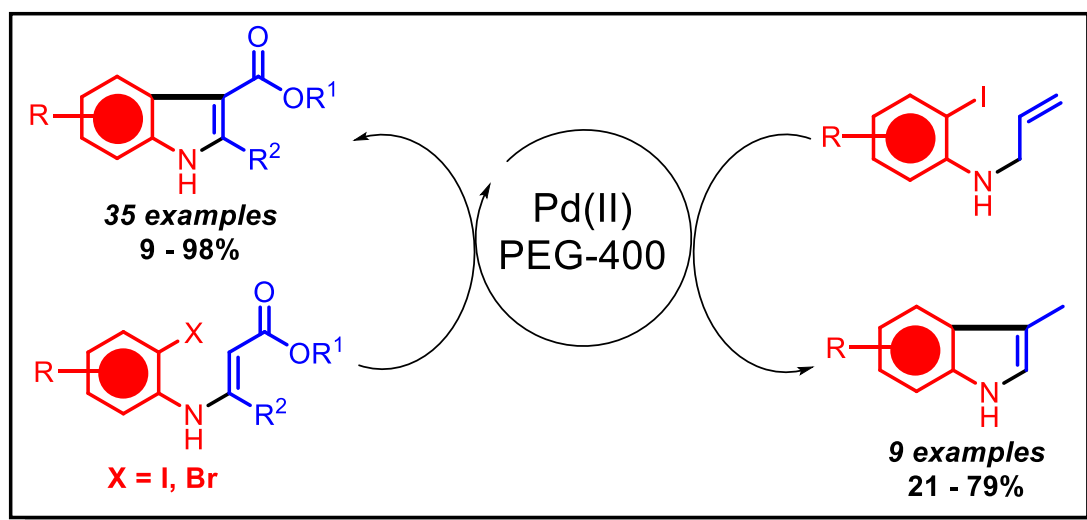


Chapter 4

Palladium (II) – PEG System for the Efficient Synthesis of Indoles *via* Intramolecular Heck Cyclisation



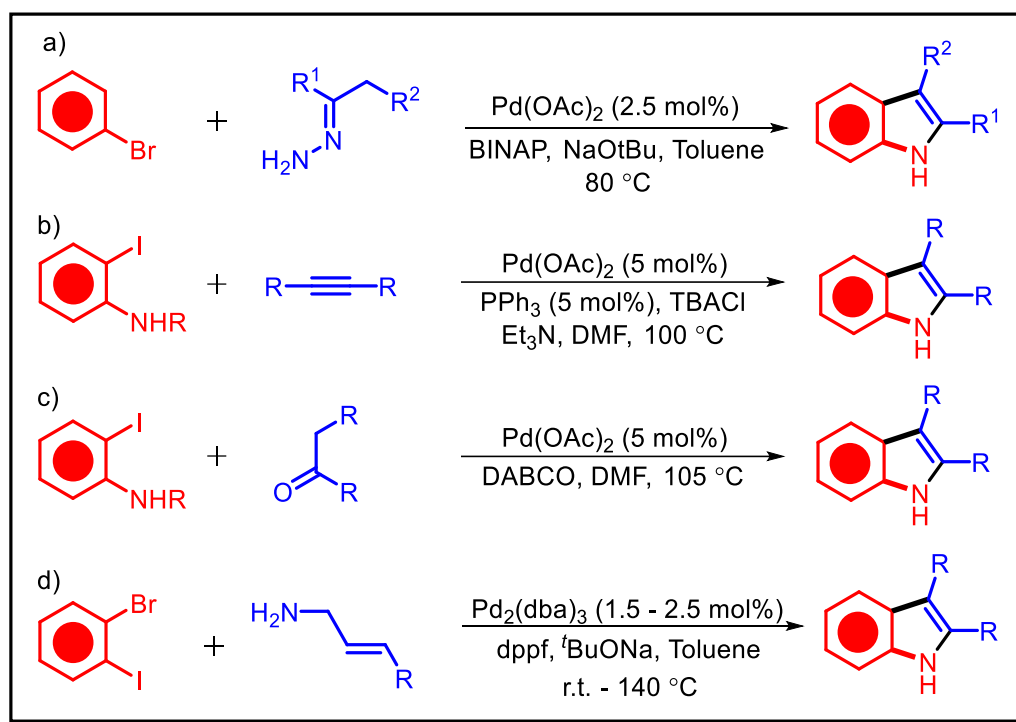
Abstract: Under palladium catalysis, *N*-vinyl-2-iodo and bromo arenes have been cyclised under milder reaction conditions, forming the indole nucleus. The cyclisable molecules (adducts) have been obtained from the Michael addition reaction of 2-haloanilines with propiolate esters. The *N*-functionalised Michael adducts have also shown cyclisability. The reaction times have been short, and yields have been consistently good to excellent. PEG-400 has played a crucial role as a solvent, enhancing the reaction efficiency. Its dual functionality as a mild reducing agent and stabiliser contributes to greener and more sustainable reaction conditions.

Palladium (II) – PEG System for the Efficient Synthesis of Indoles *via* Intramolecular Heck Cyclisation

4.1. Introduction

Transition metal-catalysed cross-coupling techniques, including the Suzuki-Miyaura, Sonogashira, Negishi, and Heck coupling processes, have become indispensable tools in synthetic organic chemistry [1]. These methodologies facilitate the formation of carbon-carbon (C-C) and carbon-heteroatom (C-X) bonds, enabling the construction of complex molecular frameworks. Among these, the Mizoroki-Heck process, which ties aryl halides (e.g., iodobenzene, bromobenzene) or vinyl halides/triflates with terminal or internal alkenes (e.g., styrene, acrylates, or olefins), stands out as particularly powerful. This reaction leverages palladium catalysts, such as $\text{Pd}(\text{PPh}_3)_4$ or $\text{Pd}(\text{OAc})_2$, often in conjunction with bases like triethylamine or potassium carbonate, and solvents such as DMF or toluene. Notably, this reaction is widely applied in synthesising small and medium-sized carbocycles and heterocycles, where it enables the selective formation of tertiary and quaternary stereocenters. To prevent undesirable *syn*- β -hydride elimination, strategies such as incorporating bulky substituents or introducing heteroatoms at the allylic position have been employed [2]. The intramolecular Heck reaction [3], where alkenes are tethered to aryl or vinyl halides within the same molecule, has emerged as a cornerstone for synthesising diverse carbocyclic and heterocyclic systems, offering unmatched precision and versatility. In the context of indole synthesis, a class of heterocycles widely recognised for their prevalence in natural products and pharmaceuticals, the development of innovative synthetic strategies remains a vibrant area of research. Indole synthesis *via* traditional acid-catalysed Fischer indole synthesis [4], which employs phenylhydrazine and ketones (e.g., acetophenone), has been foundational but often suffers from harsh conditions and limited scope. Modern alternatives, such as the Bartoli indole synthesis [5], utilise nitroarenes and vinyl Grignard reagents, while the Gassman indole synthesis [6] employs hypohalites as key reagents. The Nenitzescu reaction [7], involving *o*-nitrobenzaldehydes and enamines or enol ethers, exemplifies a transfer hydrogenation strategy.

Palladium catalysed indole synthesis, involving aryl halides has been studied by several researchers. The earlier reported Fisher protocol, for instance, under Buchwald modification using Pd(0) catalysis resulted in excellent indole yields (**Scheme 4.1(a)**) [8]. Similar protocols involving aryl iodides and a cyclisation partner such as Larock's alkyne annulation protocol (**Scheme 4.1(b)**) [9], Chen's imine protocol (**Scheme 4.1(c)**) [10] and Jorgensen's enamine protocol (**Scheme 4.1(d)**) [11] have been developed and further studied



Scheme 4.1. Palladium catalysed cyclisation strategies for indole synthesis

Intramolecular Heck reactions, particularly in the Mori-Ban indole synthesis [12], offer a robust approach where aryl halides tethered to alkenes within the same molecule undergo palladium-catalysed cyclisation. Typical conditions include the use of $\text{Pd}(\text{OAc})_2$ or $\text{Pd}(\text{PPh}_3)_4$ as the catalyst, a base like K_2CO_3 or NaOAc , and solvents such as NMP or DMF. Pioneering contributions by Hegedus [13], Larock [14], Li [15], and Hiemstra [16] have significantly advanced this field, fine-tuning reaction conditions to improve yields and stereochemical outcomes. The use of supercritical CO_2 as a green solvent, demonstrated by Carroll and colleagues [17], has further expanded the sustainability of these reactions. Moreover, the development of milder and more versatile conditions by Banwell [18] and Mao [19] groups has enabled the

synthesis of indoles under less harsh conditions, broadening the functional group tolerance and applicability of these methods. These advancements underline the importance of meticulous selection of reactants, catalysts, and reaction conditions in optimising indole synthesis and related transformations. By continuing to refine these methodologies, chemists can expand the synthetic utility of indoles and other heterocycles, supporting their applications in drug discovery, material science, and beyond.

Globally, nanoparticles have emerged as transformative materials in various scientific fields owing to their remarkably small size, high surface expanse, and the presence of multiple catalytically active sites. Among these, Pd(0) nanoparticles have demonstrated remarkable catalytic activity, significantly accelerating palladium-catalysed cross-coupling reactions, that take in the Suzuki–Miyaura and Heck reactions [20]. These reactions play a pivotal role in constructing complex molecular frameworks, including biologically active compounds and materials for industrial applications. This study explores the synthesis of the indole nucleus, a critical structural motif in pharmaceuticals and natural products, through an intramolecular Heck cyclisation of *N*-vinyl and *N*-allyl-2-iodo and 2-bromoanilines. The approach leverages nanoparticles of Pd(0) made *in-situ* as highly efficient catalysts, leading to substantially reduced reaction times and enhanced yields. The process is facilitated by the unique properties of the nanoparticles, including their high dispersibility and catalytic efficiency. Polyethylene glycol (PEG-400) is employed as the solvent in this reaction, offering distinct advantages such as high boiling point, non-volatility, and eco-friendliness. The use of PEG-400 plays a crucial role in this synthetic methodology by ensuring better solubilisation of the reactants, thereby creating a conducive environment for the reaction to proceed efficiently. Additionally, PEG-400 facilitates the stabilisation of Pd nanoparticles, eliminating the necessity for external stabilising agents or ligands [21]. This reaction, which utilises *N*-vinylated and *N*-allylated aniline derivatives as substrates, demonstrates an intramolecular coupling under mild conditions, resulting in the formation of the indole core (**Scheme 4.1**), a vital structure in many biologically active compounds. Notably, this method significantly reduces reaction times compared to conventional protocols while simplifying the overall process. The reliance on Pd(0) nanoparticles within this framework underscores their remarkable versatility and efficiency as catalysts, enabling greener,

faster, and more cost-effective synthetic strategies. Furthermore, the approach aligns with the principles of sustainable chemistry, offering a more economical alternative with potential scalability for industrial applications. This methodology holds significant promise for large-scale drug synthesis and the development of functional materials, further exemplifying the transformative role of nanoparticles in advancing modern organic chemistry.

4.2. Objectives of the present work

Chapter 4 has been divided into two sub-chapters namely Chapter 4a and Chapter 4b where following essential organic transformations have been carried out:

- (i) Chapter 4a deals with the synthesis of indoles *via* the intramolecular Heck cyclisation of the adducts of 2-iodoaniline with propiolate esters and allyl bromides using the Pd(II)-PEG system. Polyethylene glycol – 400 (PEG-400) owing to its abilities as a good solubiliser of the reactants and a stabiliser has facilitated the high activity of the reaction system in the transformation.
- (ii) Chapter 4b deals with the cyclisation of *N*-vinyl-2-bromoanilines to form indoles using the Pd(II)–PEG system. Additionally, studies related to the scalability and one pot synthesis are also major objectives of the study.

4.3. Experimental section

4.3.1. General Information

All the starting materials were purchased commercially and were used without further purification. All the Michael adducts were synthesised in 100 mL round bottom flasks. All reactions related to the synthesis of indoles were performed inside round bottom flasks (50 mL, Borosil™) and Sealed Tubes (VENSIL™) under ambient conditions. TLC plates (Silica gel 60-F254 coated on aluminium plates purchased from Merck) were visualised by either UV light or inside an iodine chamber. ¹H and ¹³C NMR experiments were performed using JEOL ECS-400MHz and Bruker Avance III 500 MHz spectrometers. The chemical shifts were quoted in reference to tetramethyl silane (for ¹H) and CDCl₃ (for ¹³C NMR) as internal standards.

4.3.2. Single crystal X-ray diffraction studies

Single crystal X-ray diffraction studies were performed using a single crystal directly obtained from the reaction mixtures. Diffraction data for the compounds were collected on a Bruker APEX-II CCD Diffractometer with MoK α radiation ($\lambda = 0.71073$ Å), employing φ and ω scans of narrow (0.5°) frames at 100 K. The structure was determined using direct methods with SHELXL-97, as implemented in the WinGX program system [1]. Anisotropic refinement was applied to all non-hydrogen atoms, while aliphatic and aromatic hydrogen atoms were positioned based on calculated locations and allowed to ride on their parent atoms during subsequent refinement cycles.

4.3.3. General procedure for the Michael addition of 2-Haloanilines with propiolate esters

The 2-((2-halophenyl)amino)maleate derivatives (**3**) were synthesised as per the following literature procedure [1]. A thoroughly cleaned and oven dried round bottom flask (RB, 100 mL) was charged with 1 equivalent (5 mmol) of 2-haloanilines (**1**) and 1 equivalent (5 mmol) of the propiolate esters (**2**) in 20 mL methanol at room temperature under ambient aerial conditions. The reaction was allowed to stir at 40 °C for 1 hour (monitored using TLC). Upon completion (as indicated by TLC), methanol was evaporated under vacuum followed by extraction with ethyl acetate (3 x 20 mL). The combined organic layers were washed with brine, dried using anhydrous Na₂SO₄ and concentrated in vacuum. The crude product was purified using silica gel column chromatography (1%-3% EtOAc-Hexanes) as the eluent to afford the pure products (**Scheme 4.2**).

4.3.4. General procedure for the *N*-functionalisation of the adducts

In a clean 100 mL round bottom flask 2 mmols of the Michael adduct (**3**), 2 equivalents of a non-nucleophilic base (NaH) and 2 equivalents of the alkyl/benzyl halide were taken in the presence of 15 mL dry DMF as solvent. The reaction mixture was stirred at room temperature and the reaction was monitored using thin layer chromatography. After completion, the reaction was poured into 250 mL ice water and was extracted with ethyl acetate several times. The combined organic layers were

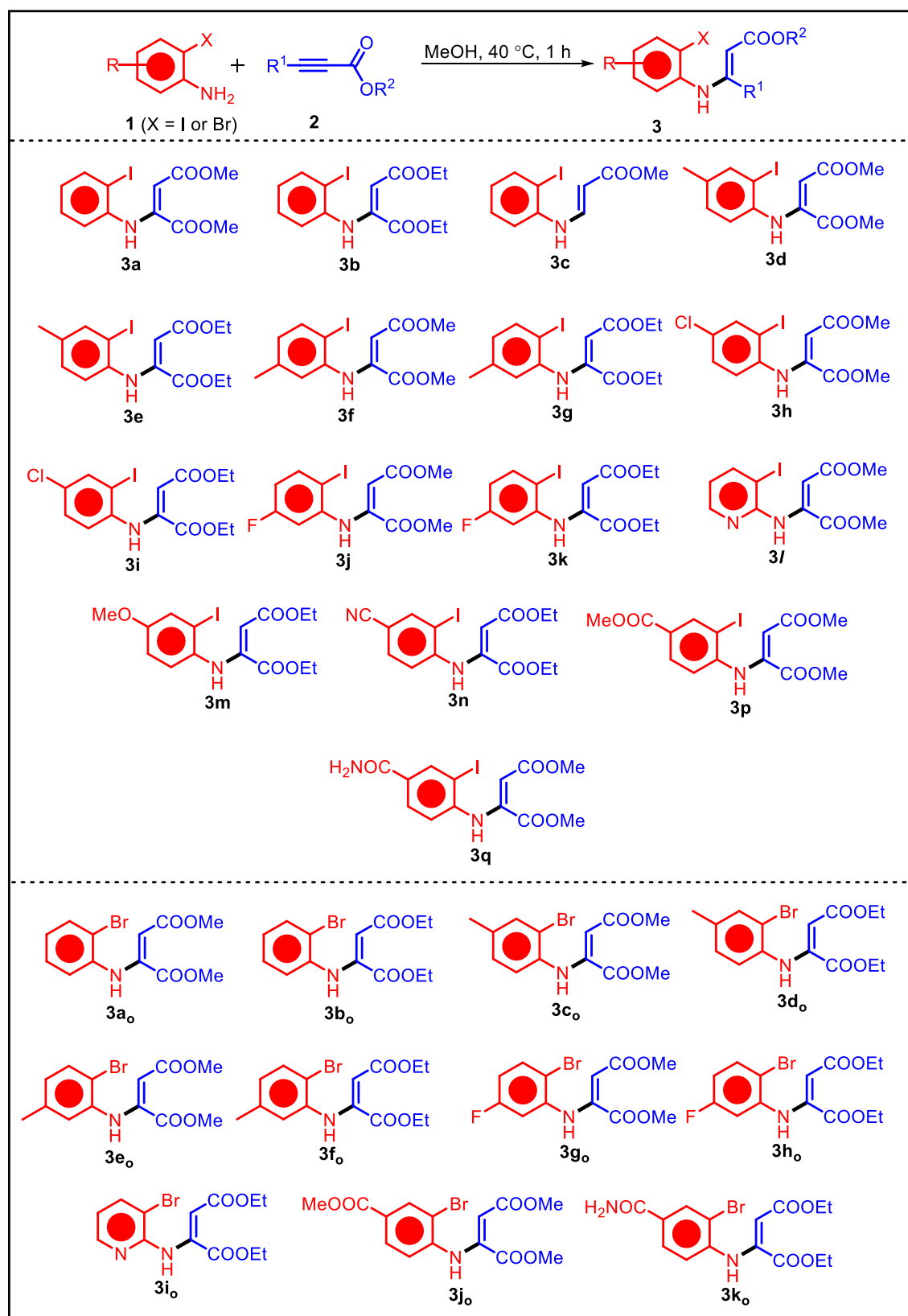
then washed with brine and dried with sodium sulfate. Subsequent column chromatography yielded the products (**4**) (**Scheme 4.3**).

4.3.5. General procedure for the *N*-allylation of 2-iodoanilines

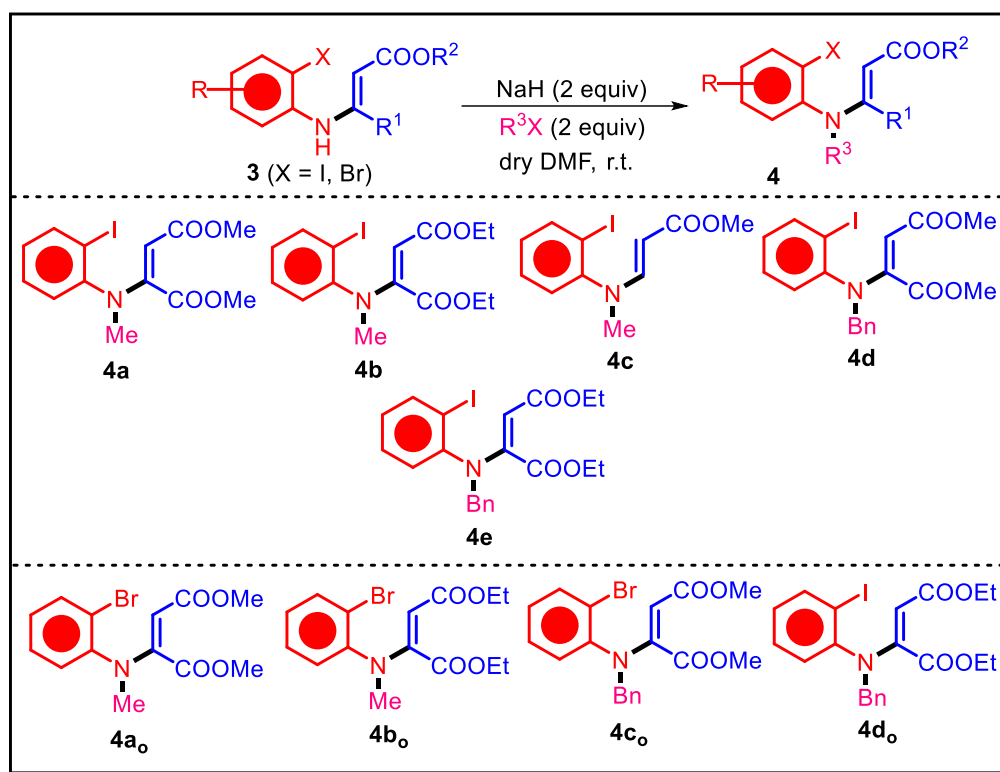
In a clean and dried round-bottom flask, 1 equivalent (5 mmol) of 2-haloaniline, allyl bromide, K_2CO_3 , and 10 mL of *N,N*-dimethylformamide (DMF) solvent were combined. The reaction mixture was stirred at 50 °C for 5 hours, with progress monitored by thin-layer chromatography (TLC). Upon completion (as indicated by TLC), the reaction mixture was poured into 100 mL of ice water and extracted with ethyl acetate. The combined organic layers were washed with brine, dried over anhydrous sodium sulfate, and concentrated under vacuum to yield the crude product. Purification *via* silica gel column chromatography (100–200 mesh silica gel) using hexanes as the eluent afforded the product. Using 1.1 equivalent of allyl bromide and 2 equivalents of K_2CO_3 yields *N*-allyl-2-haloaniline, while using 3 equivalents of allyl bromide and 3 equivalents of K_2CO_3 results in *N,N*-diallyl-2-haloaniline due to further substitution on the nitrogen atom (**Scheme 4.4**).

4.3.6. General procedure for the synthesis of *N*-alkyl-*N*-allyl-2-iodoanilines from *N*-allyl-2-iodoanilines

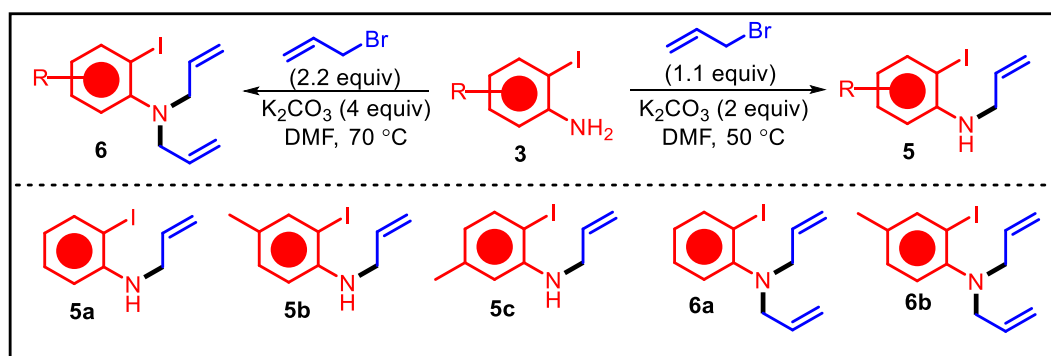
1 equivalent of *N*-allyl-2-iodoanilines (**5**) synthesised as per **Scheme 4.4** were taken in a round bottom flask and allowed to react with 2 equivalents of sodium hydride and 1.1 equivalents of methyl iodide and 2 equivalents of benzyl bromide at room temperature for 4 hours. After completion of the reaction (as per TLC), the reaction mixture was poured into ice water and was extracted with ethyl acetate. The combined organic layers were washed with brine and dried with anhydrous sodium sulfate and concentrated under reduced pressure. Purification *via* silica gel column chromatography (100–200 mesh silica gel) using hexanes as the eluent afforded the product (**7**) (**Scheme 4.5**).



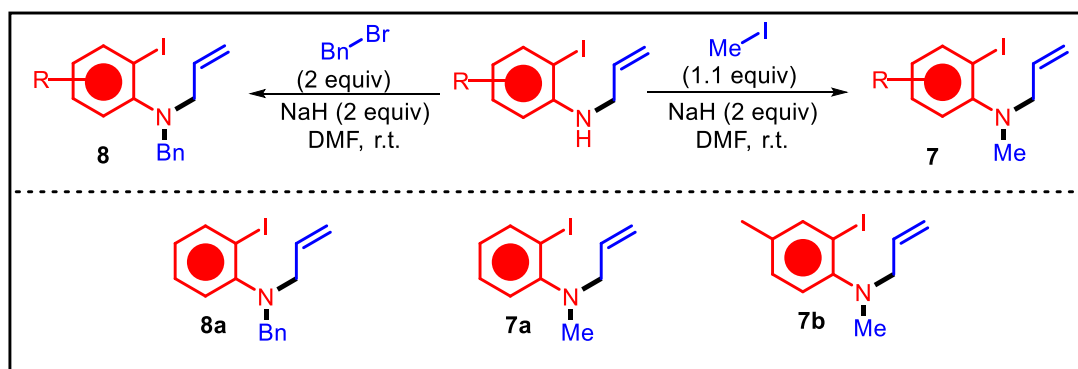
Scheme 4.2. Synthesis of 2-haloaniline – propiolate ester adducts



Scheme 4.3. N-arylation of 2-haloaniline and propiolate ester adducts



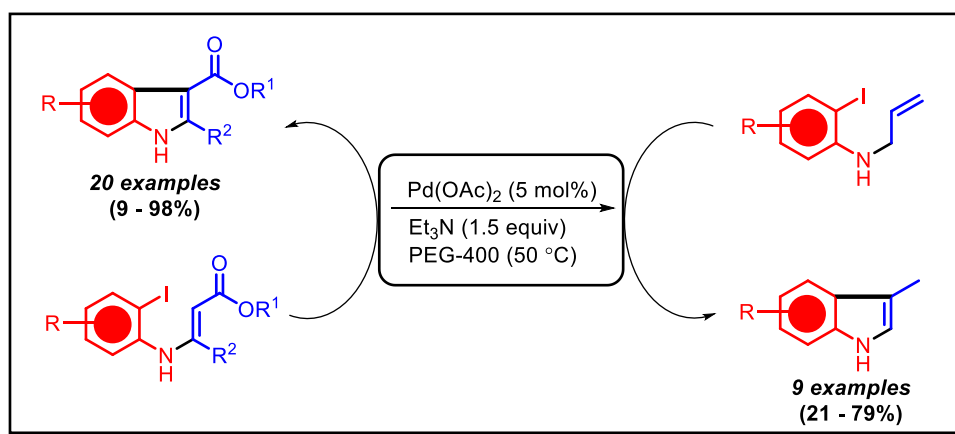
Scheme 4.4. Synthesis of N-allyl and N,N-diallyl-2-iodoanilines



Scheme 4.5. N-alkylation of N-allyl-2-iodoanilines

Chapter 4a

***In-Situ* Generated Palladium Nanoparticles Catalysed Synthesis of Indoles *via* Intramolecular Heck Cyclisation of *N*-vinyl and *N*-allyl-2-iodoanilines**



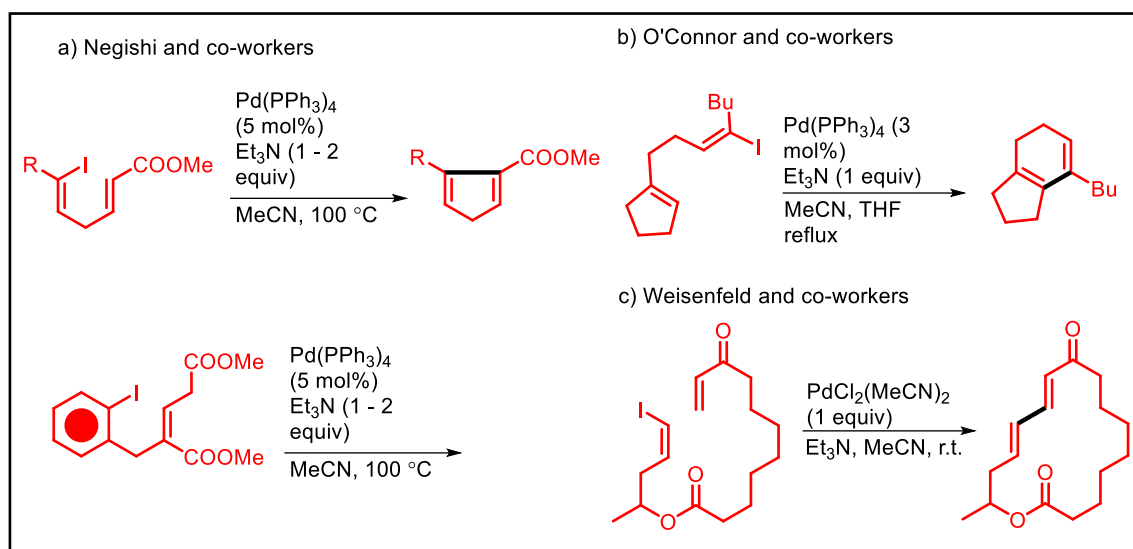
Abstract: Under palladium catalysis, *N*-vinyl-2-iodo and *N*-allyl-2-iodo arenes undergo cyclisation under gentler conditions, leading to the formation of indole frameworks. These cyclisable intermediates (adducts) are synthesised through the Michael addition reaction of 2-iodoanilines with propiolate esters. Importantly, the *N*-functionalised Michael adducts also display the ability to cyclise. The reactions are characterised by short durations and consistently high to excellent product yields. The catalytic process owes its efficiency to the *in-situ* generation of palladium nanoparticles, with PEG-400 functioning as both a reducing agent and a stabiliser for the nanoparticles. Moreover, this system operates as a heterogeneous catalyst and retains its activity for up to three reuse cycles.

***In-Situ* Generated Palladium Nanoparticles Catalysed Synthesis of Indoles *via* Intramolecular Heck Cyclisation of *N*-vinyl and *N*-allyl-2-iodoanilines**

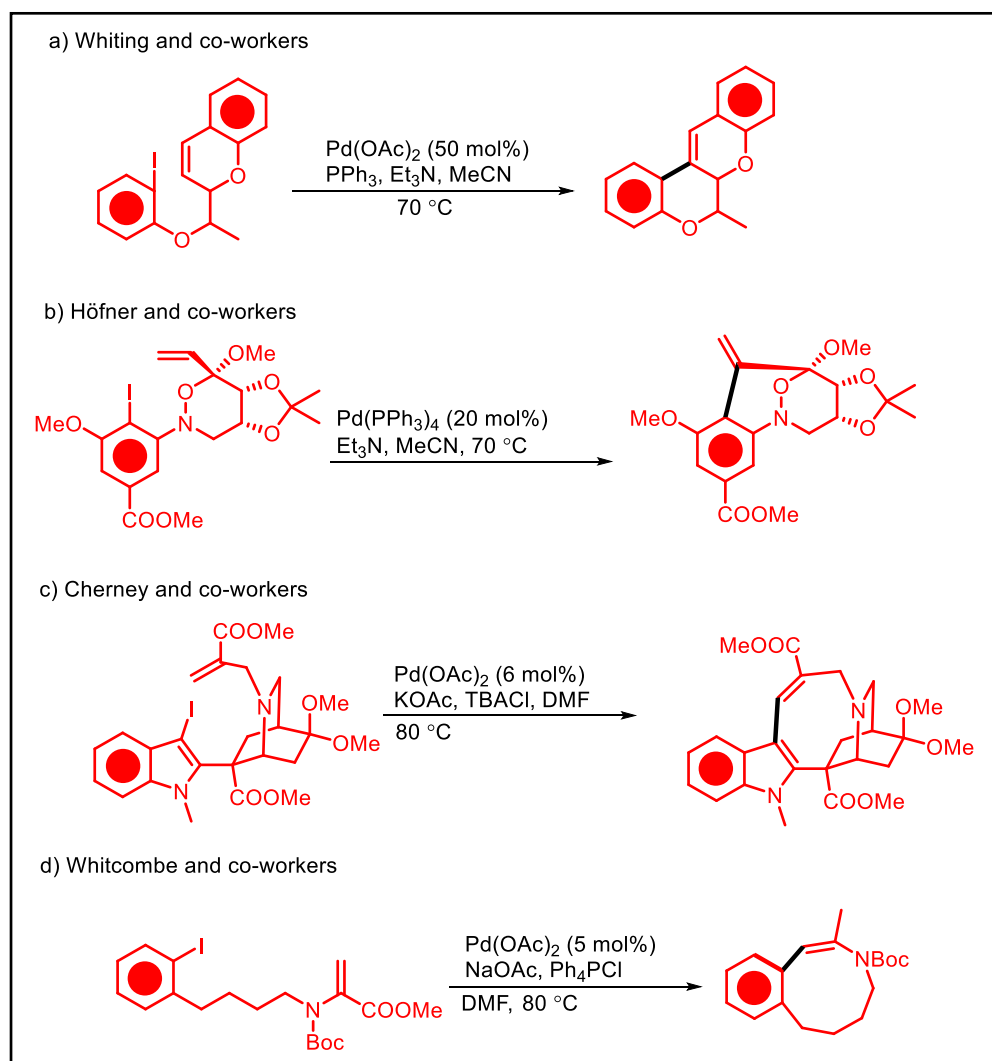
4.4. Introduction

Palladium has become essential in organic chemistry due to its ability to mediate diverse reactions *via* redox cycling between Pd(0) and Pd(II) states, with standard reduction potentials around +0.951 V to +0.987 V (versus SHE) [21]. This flexibility drives key steps like oxidative addition and reductive elimination, enabling efficient cross-coupling reactions for precise bond formation. Among these, an important cross-coupling reaction is the Heck reaction. The Heck reaction, a vital tool in organic synthesis, enables the coupling of olefins with aryl or vinyl groups. Traditionally, it employs palladium-based catalysts with aryl bromides and iodides as standard substrates. Over time, the reaction has expanded to accommodate diverse arylating agents [20]. The intramolecular Heck reaction has become a versatile tool for synthesising carbocyclic and heterocyclic compounds. It has been widely employed to construct small, medium, and large carbocyclic rings, as illustrated by the works of Negishi [22], Masters [23], O'Connor [24], and Weisenfeld [25] groups (**Scheme 4.6**). Additionally, it has been instrumental in the formation of heterocyclic rings, with significant contributions from researchers such as Whiting, Hofner, Cherney, and Whitcombe groups (**Scheme 4.7**). Notably, this process has also been effectively utilised in the generation of privileged indole nucleus [26], as demonstrated by Larock [14], Mao [19], Yamanaka [29], Mengeneay [30], and Banwell [18] and co-workers (**Scheme 4.8**), further establishing its status as a benchmark for C–C bond formation.

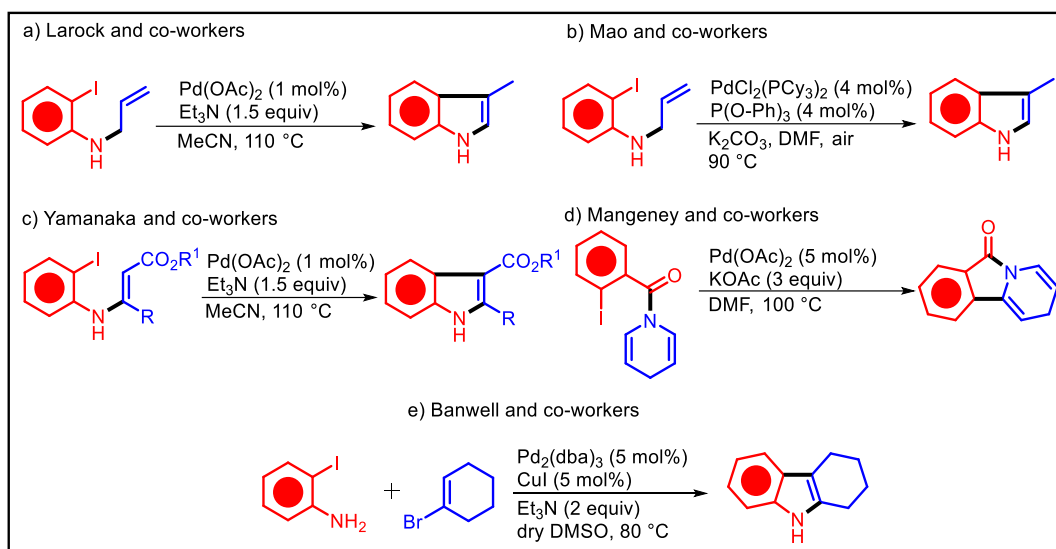
In recent developments, palladium nanoparticles have emerged as a superior alternative to conventional catalysts. Their high surface-area-to-volume ratio significantly enhances catalytic efficiency, while their heterogeneous nature allows for easier recovery and reuse. These nanoparticles not only improve reaction sustainability but also broaden the Heck reaction's applications, particularly in pharmaceutical production, materials development, and green chemistry initiatives [27].



Scheme 4.6. Intramolecular Heck cyclisation for the synthesis of carbocycles



Scheme 4.7. Intramolecular Heck cyclisation for the synthesis of heterocycles



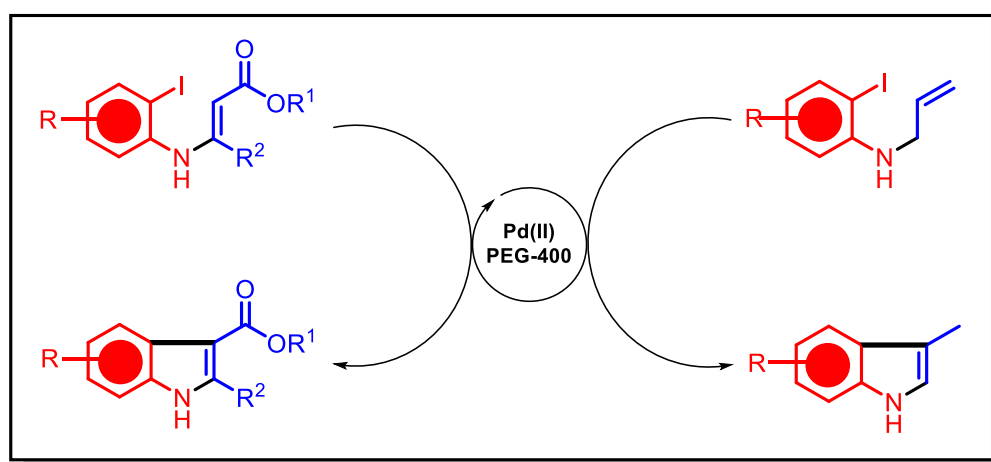
Scheme 4.8. Intramolecular Heck cyclisation for the synthesis of indoles

The *in-situ* generation of nanoparticles from transition metal salts has emerged as an efficient strategy to accelerate reaction rates by acting as active catalysts for chemical transformations. This approach utilises freshly formed nanoparticles with high surface areas and abundant active sites, enhancing catalytic efficiency while avoiding aggregation. By eliminating the need for pre-synthesised catalysts, it simplifies processes, reduces costs, and saves time. Additionally, it often enables milder reaction conditions, improves selectivity, yield, and scalability, and minimises waste and the use of harsh reagents, making it an eco-friendly and sustainable option for organic synthesis. Such strategies of *in-situ* nanoparticle generation have been successfully employed in various important organic reactions. In cross-coupling reactions like Suzuki, Sonogashira, and Heck reactions, *in-situ*-generated nanoparticles act as efficient catalysts, facilitating C-C bond formation with high selectivity and efficiency. These reactions are vital in the synthesis of pharmaceuticals, agrochemicals, and materials. Additionally, *in-situ* catalysis is effective in oxidation and reduction reactions, offering improved reaction rates and milder conditions. The flexibility and robustness of these strategies make them increasingly popular in green chemistry and sustainable organic synthesis [28].

A key factor in regulating the size, stability, and catalytic characteristics of *in-situ* nanoparticles is the solvent choice. Aqueous solutions, which are safe for the environment and aid in stabilising ionic species; alcohols like ethanol and methanol, which can also be used as mild reducing agents; polar aprotic solvents like

acetonitrile, DMF, and DMSO, which dissolve metal salts and facilitate the dispersion of nanoparticles; ionic liquids, which offer tunable properties and enhanced stability for nanoparticles; solvent-free systems, which use substrates as the reaction medium, which reduce waste; and polyols, such as ethylene glycol and glycerol, which are especially good at stabilising nanoparticles because of their high boiling points and effective reduction of metal salts. Polyols such as polyethylene glycol (PEG) work very well to produce nanoparticles *in-situ*. PEG's hydrophilic properties and high molecular weight help stabilise nanoparticles by limiting their size and preventing aggregation. It is a versatile option for the synthesis of nanoparticles due to its solubility in both organic solvents and water. PEG promotes the regulated reduction of metal salts to nanoparticles while guaranteeing their dispersion by acting as a stabilising and reducing agent. In addition to improving nanoparticle stability and preventing agglomeration, PEG-coated nanoparticles exhibit enhanced biocompatibility, which makes them perfect for use in industrial processes, biomedical sectors, and catalysis [21].

Here, *N*-vinyl and *N*-allyl-2-iodoanilines have been intramolecularly Heck cyclised using the Pd(II)-PEG-400 system (**Scheme 4.9**). Palladium nanoparticles are produced in situ in the reaction media, which increases catalytic activity and promotes effective C-C bond formation. This method guarantees the catalyst's high activity and heterogeneity in addition to increasing the rate of reaction. The system's heterogeneity makes it simple to separate and recycle the catalyst, which increases the process's sustainability and economy.



Scheme 4.9. Pd(II)-PEG-400 system for C-C bond formation – indole synthesis

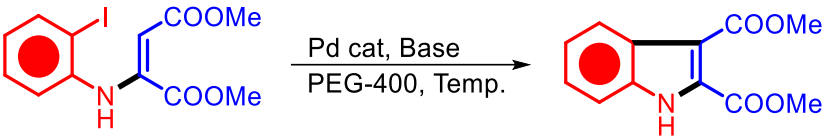
4.5. Results and discussion

4.5.1. Optimisation of the reaction conditions for the cyclisation of 2-iodo-*N*-vinylanilines

We began our optimisation studies by selecting the intramolecular cyclisation of dimethyl 2-((2-iodophenyl)amino)maleate (**4a**) as the model reaction. Initially, treating 1 equivalent (0.2 mmol) of **4a** with Palladium acetate (Pd(OAc)₂) in the company of 2 equivalents (0.2 mmol) of triethylamine (Et₃N) in PEG-400 solvent brought about the isolation of the desired product, dimethyl 1*H*-indole-2,3-dicarboxylate (**9a**), with a 91% yield after 5 hours at 110 °C (**Table 4.1, Entry 1**). Several synthetic experiments were conducted to increase the yield of the desired product further. A small increase to 92% yield was observed by lowering the temperature to 90 °C (**Table 4.1, Entry 2**). Reducing the temperature further to 60 °C, while keeping other conditions constant, increased the yield to 97% after 3.5 hours (**Table 4.1, Entry 3**). A further drop to 50 °C led to a minimal yield increase to 98% after the same time interval (**Table 4.1, Entry 4**), likely due to a reduction in protodehalogenation. Interestingly, reducing the base (Et₃N) amount to 1.5 equivalents at 50 °C did not change the yield (**Table 4.1, Entry 5**), prompting further exploration of lower amounts of Et₃N. Using 1 equivalent of triethylamine resulted in a yield decrease to 91% (**Table 4.1, Entry 6**), and a further reduction to 0.5 equivalents caused the yield to drop to 84% (**Table 4.1, Entry 7**) under identical reaction conditions. Additionally, using a lower catalyst loading of 2.5 mol% led to yields of 80% and 72% with 2 and 1.5 equivalents of Et₃N, respectively (**Table 4.1, Entries 8 and 9**). Performing the reaction at room temperature with the conditions in **Table 4.1, Entry 5**, resulted in a 75% yield after 5 hours (**Table 4.1, Entry 10**). Replacing Pd(OAc)₂ with PdCl₂ (5 mol%) also produced good yields: 95% with 1.5 equivalents of Et₃N, and a drop to 90% when the Et₃N amount was reduced to 1 equivalent after 3.5 hours (**Table 4.1, Entries 11 and 12**). When the reaction was carried out under the same conditions as **Table 4.1, Entry 11**, but at room temperature, the yield dropped to 70% (**Table 4.1, Entry 13**). Using 1.5 equivalents of potassium carbonate in place of triethylamine resulted in no product formation under the given conditions, with the starting material (**4a**) isolated intact at both 50°C and 80°C (**Table 4.1, Entries 14 and 15**). Another set of experiments, investigating

the effect of organic bases other than triethylamine, highlighted the superiority of triethylamine. When DABCO (1.5 equivalents) or DBU (1.5 equivalents) were used, the reaction proceeded sluggishly, yielding only 24% and 32% of the product in 5 hours, respectively (**Table 4.1, Entries 16 and 17**). Additionally, when a natural base, Water Extract of Banana Peel Ash (WEB), was used, only a trace amount of product was obtained (**Table 4.1, Entry 18**). Control experiments (**Table 4.1, Entries 19 and 20**) confirmed the necessity of both Palladium and triethylamine for the transformation. Conducting the reaction with Pd(OAc)₂ as well as PdCl₂ at room temperature also led to a fall in the product yield (**Table 4.1, Entries 21 and 22**). The optimised reaction conditions can therefore be shown as: 4a (1 equiv), Pd(OAc)₂ (5 mol%), Et₃N (1.5 equiv), PEG-400, 50 °C for 3 hours.

Table 4.1. Optimisation of the reaction conditions: cyclisation of **3a** to **9a**

						
Sl.	Pd catalyst (5 mol%)	Base (equiv.)	Solvent	Temp	Time (h)	Yield (%)
1	Pd(OAc) ₂	Et ₃ N (2)	PEG-400	110 °C	5	91%
2	Pd(OAc) ₂	Et ₃ N (2.)	PEG-400	90 °C	3.5	92%
3	Pd(OAc) ₂	Et ₃ N (2)	PEG-400	60 °C	3.5	97%
4	Pd(OAc) ₂	Et ₃ N (2)	PEG-400	50 °C	3.5	97%
5	Pd(OAc)₂	Et₃N (1.5)	PEG-400	50 °C	3	98%
6	Pd(OAc) ₂	Et ₃ N (1)	PEG-400	50 °C	3.5	91%
7	Pd(OAc) ₂	Et ₃ N (0.5)	PEG-400	50 °C	3.5	84%
8	Pd(OAc) ₂	Et ₃ N (2)	PEG-400	50 °C	5	80% ^c
9	Pd(OAc) ₂	Et ₃ N (1.5)	PEG-400	50 °C	6	72% ^c
10	Pd(OAc) ₂	Et ₃ N (1.5)	PEG-400	r.t.	5	75%
11	PdCl ₂	Et ₃ N (1.5)	PEG-400	50 °C	3.5	95%
12	PdCl ₂	Et ₃ N (1)	PEG-400	50 °C	3.5	90%
13	PdCl ₂	Et ₃ N (1.5)	PEG-400	r.t.	4	70%
14	Pd(OAc) ₂	K ₂ CO ₃ (1.5)	PEG-400	50 °C	5	NR

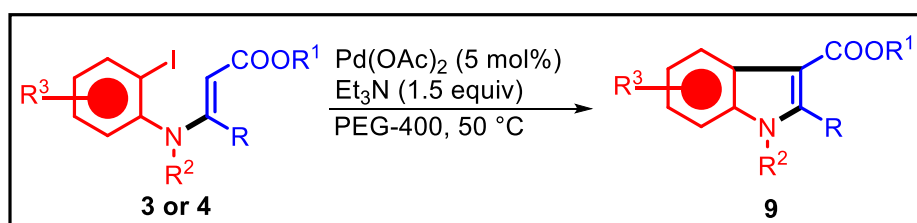
15	Pd(OAc) ₂	K ₂ CO ₃ (1.5)	PEG-400	80 °C	5	NR
16	Pd(OAc) ₂	DABCO (1.5 eq.)	PEG-400	50 °C	5	24%
17	Pd(OAc) ₂	DBU (1.5 eq)	PEG-400	50 °C	5	32%
18	Pd(OAc) ₂	WEB (1 mL)	PEG-400	50 °C	6	Trace
19	-	Et ₃ N (1.5 eq.)	PEG-400	50 °C	5	NR
20	Pd(OAc) ₂	-	PEG-400	50 °C	5	NR
21	Pd(OAc) ₂	Et ₃ N (1.5 eq.)	PEG-400	r.t.	7	76%
22	PdCl ₂	Et ₃ N (1.5 eq.)	PEG-400	r.t.	7	72%

Reaction conditions: **3a** (1 eq., 0.2 mmol), Pd(OAc)₂ (5 mol%), PEG (1 mL) (Inside a sealed tube), ^aX=I, ^bX=Br, ^cPd(OAc)₂ (2.5 mol%), WEB (Water extract of Banana peel ash), NR (no result).

4.5.2. Substrate scope studies

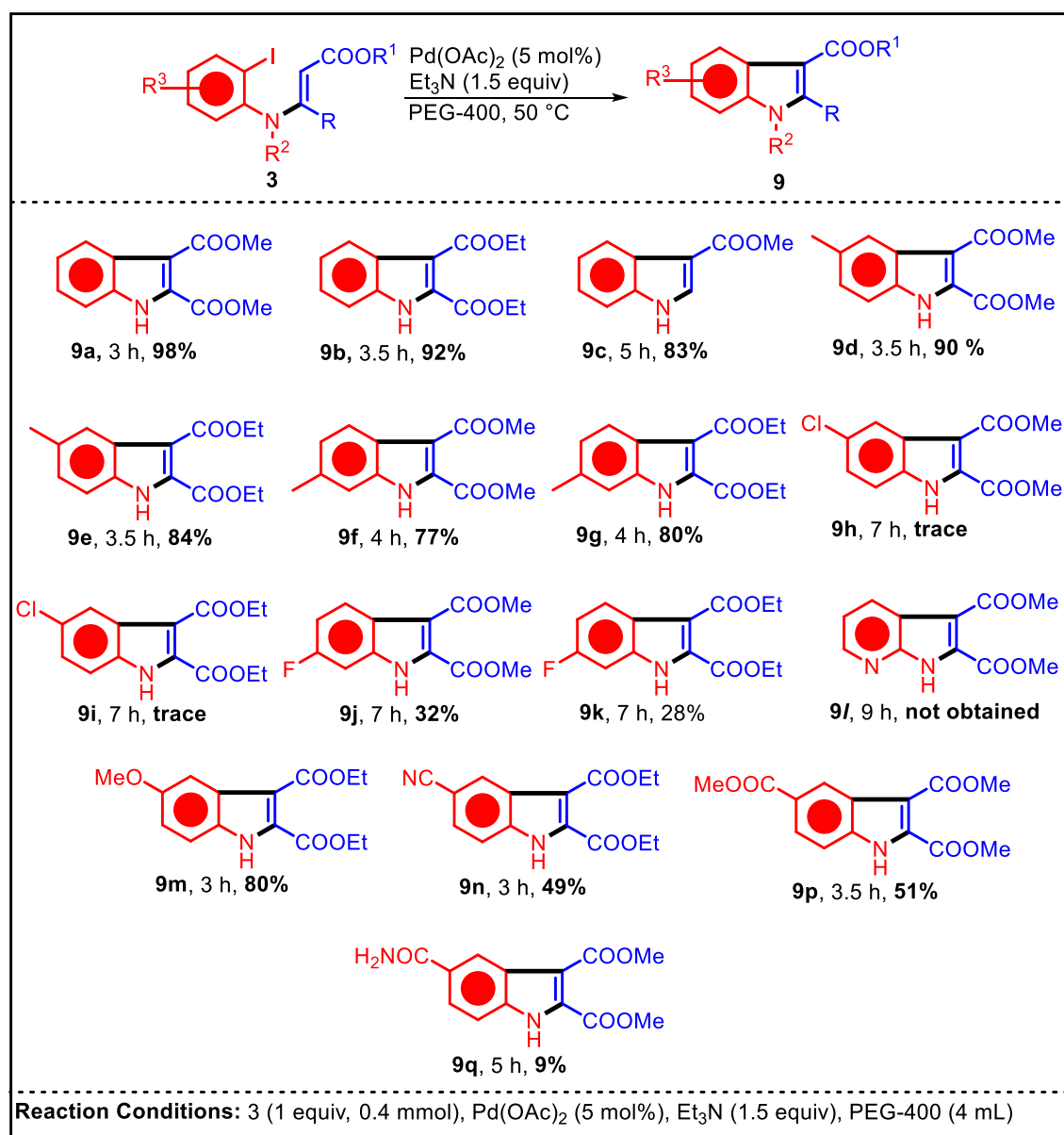
4.5.2.1. General procedure for the cyclisation of the 2-iodo-*N*-vinylanilines and 2-iodo-*N*-allylanilines

All the substrates were cyclised on a 0.3 mmol (1 equiv) scale as per the following procedure. A thoroughly cleaned and round bottom flask was charged with 1 equivalent (0.1 mmol) of 2-((2-iodophenyl)amino)maleate, 5 mol% of Palladium acetate catalyst and 1.5 equivalents of triethyl amine (anhydrous) in PEG-400 solvent (1.5 mL). The reaction mixture was allowed to stir at 50 °C for 3 hours (monitored *via* TLC). Upon completion, the reaction was quenched with a saturated solution of ammonium chloride, filtered through a plug of celite and was extracted with Ethyl acetate (3 x 20 mL). The combined organic layers were washed with brine and dried using anhydrous sodium sulphate and concentrated in vacuum to get the crude product. The crude mixture was purified using silica gel column chromatography (60-120 silica gel) in 10%-20% EtOAc–Hexanes as the eluent to afford the pure indole products (**Scheme 4.10**).

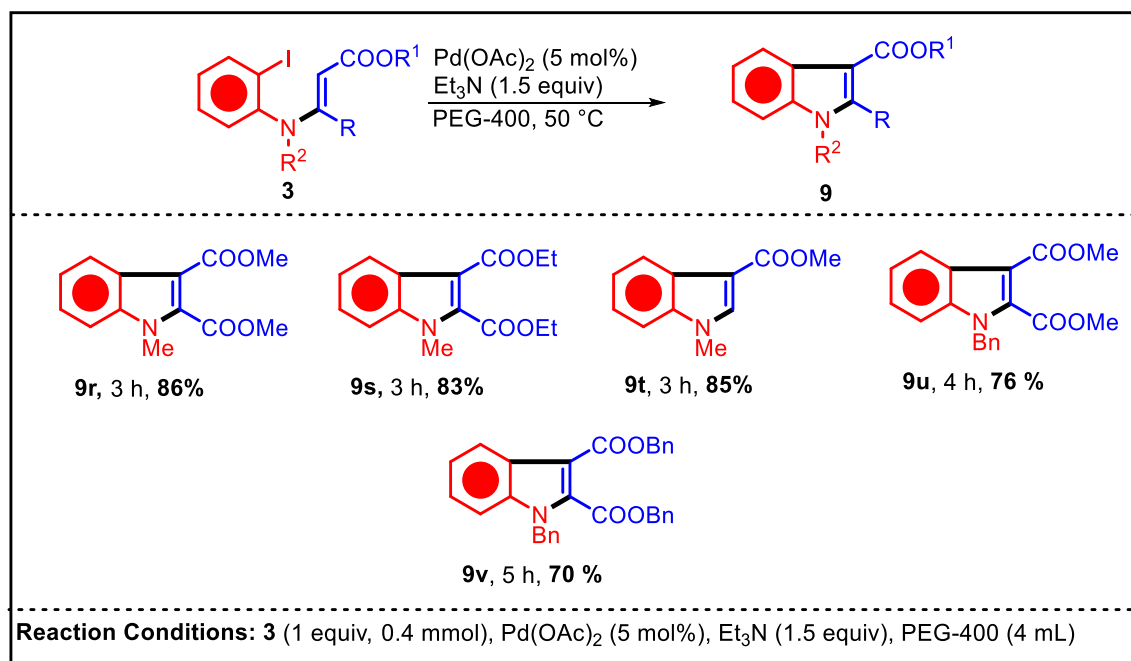


Scheme 4.10. Cyclisation of 2-iodo-*N*-vinylanilines using Pd(II)-PEG system4.5.2.2. Substrate scope studies for the cyclisation of 2-iodo-*N*-vinylanilines and *N*-functionalised-2-iodo-*N*-vinylanilines

After optimising the reaction conditions, we explored the substrate scope using various electronically diverse adducts, as summarised in **Table 4.2**. The cyclisation of the adduct of 2-iodoaniline and dimethyl acetylene dicarboxylate (DMAD) (**3a**) afforded product **9a** in an impressive 98% yield within 3 hours. Similarly, the cyclisation of the adduct of 2-iodoaniline and diethylacetylene dicarboxylate (DEAD) (**3b**) yielded indole product **9b** with a favorable 92% yield in 3 hours. Cyclisation of the adduct **3c** produced **9c** in 83% yield. The adducts of 2-iodo-4-methylaniline with DMAD and DEAD (**3d** and **3e**) afforded products **9d** and **9e** with yields of 90% and 84%, respectively. However, lower yields were observed when 2-iodo-5-methylaniline was used instead of 2-iodo-4-methylaniline, with cyclisation of adducts **3f** and **3g** (with DMAD and DEAD) yielding **9f** and **9g** at 80% and 77%, respectively. Under the same reaction conditions, the cyclisation of adducts derived from 4-chloro-2-iodoaniline with DMAD and DEAD (**3h** and **3i**) produced trace amounts of products **5h** and **5i**. Attempts to cyclise adducts of 5-fluoro-2-iodoaniline with DMAD (**3j**) and DEAD (**3k**) resulted in products **9j** (32% in 7 hours) and **9k** (28% in 7 hours). Cyclisation of the adduct of 2-amino-3-iodopyridine failed to yield **9l**, likely due to coordination of the palladium center with the aminopyridyl system. Cyclisation of the adduct of 4-methoxy-2-iodoaniline with DMAD afforded **9m** in 80% yield within 3 hours. Similarly, cyclisation of adducts derived from 4-cyano-2-iodoaniline and 4-carboxy-2-iodoaniline methyl ester with DMAD produced **9n** (49% in 3 hours) and **9p** (51% in 3.5 hours), respectively. Cyclisation of the adduct of 4-amido-2-iodoaniline with DMAD resulted in a low yield of **9q** (9%).

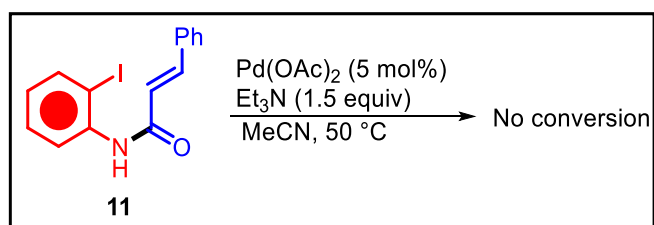
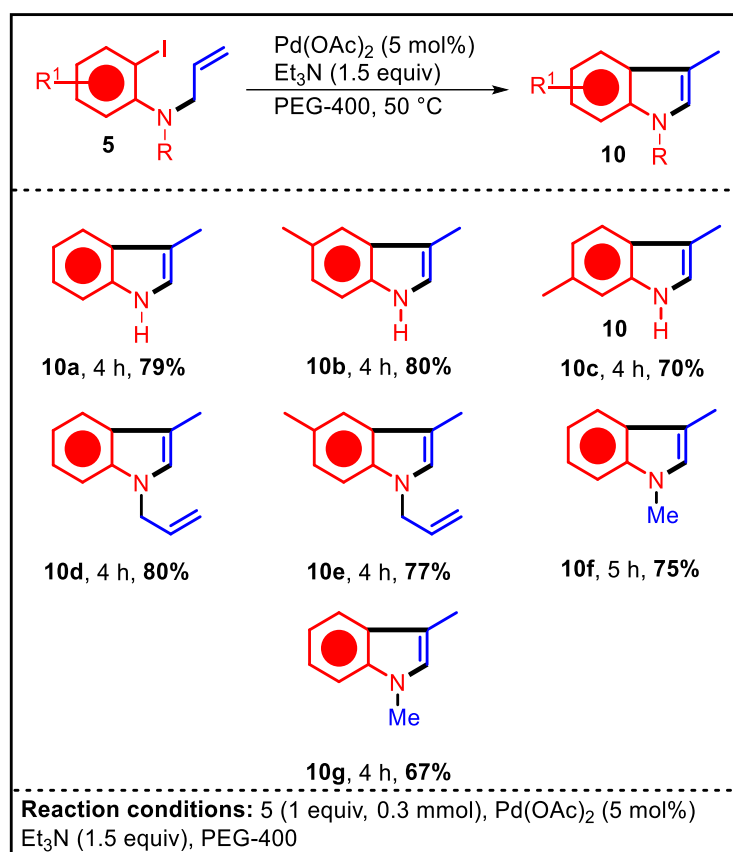
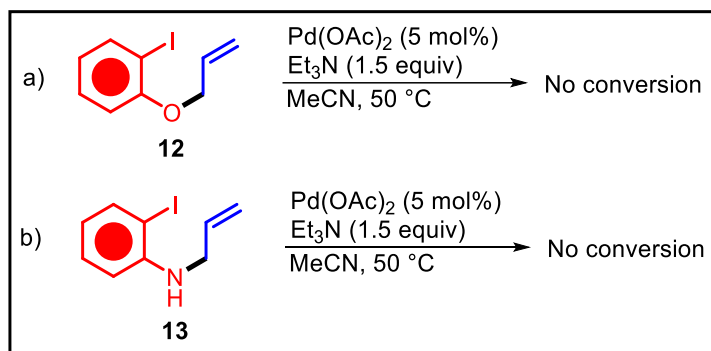
Table 4.2. Substrate scope studies for Heck cyclisation of *N*-unprotected adducts4.5.2.2. Substrate scope studies for the cyclisation of 2-iodo-*N*-allylanilines

The substrate scope studies, outlined in **Table 4.3**, were extended to investigate the cyclisation of *N*-allyl-2-iodoanilines (**Table 4.4**). These compounds were found to undergo cyclisation under similar conditions as *N*-vinyl-2-iodoanilines. The primary product of *N*-allyl-2-iodoaniline (**5a**) cyclisation was identified as 3-methyl-substituted indole (**10a**), obtained in a 79% yield. This led to the synthesis of a series of 3-methyl-substituted indoles.

Table 4.3. Substrate scope studies for Heck cyclisation of *N*-protected adducts

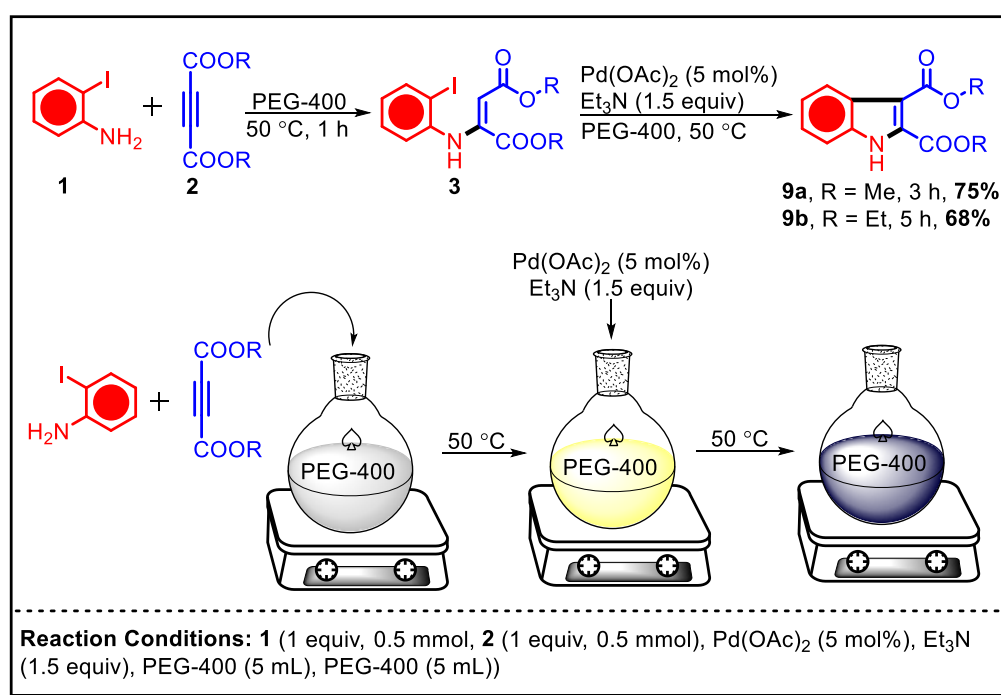
The cyclisation of *N*-allyl-2-iodo-4-methylaniline (**5b**) resulted in a yield of 80% of product **10b** in 4 hours, while the cyclisation of *N*-allyl-2-iodo-5-methylaniline (**5c**) produced 70% of product **10c** in 4 hours. Similarly, the cyclisation of *N*, *N*-diallyl-2-iodoaniline (**6a**) yielded 80% of product **10d** in 4 hours, and *N*, *N*-diallyl-2-iodo-4-methylaniline (**6b**) afforded 77% of product **10e** in 4 hours. Subsequently, the cyclisation of *N*-allyl-*N*-methyl-2-iodo-4-methylaniline (**7a**) produced 75% yield of indole **10f** in 5 hours, whereas *N*-allyl-*N*-benzyl-2-iodo-4-methylaniline (**8a**) yielded 67% of the product **10g** in 4 hours. Notably, the addition of 20 mol% PPh₃ resulted in a 1-2% increase in yield across all cases (**Table 4.3**).

Moreover, cyclisation of *N*-cinnamoyl-2-iodoaniline (**11**) did not yield any desired product, with the starting material being recovered unchanged. These findings are summarised in **Table 4.4**. Additionally, *O*-allyl-2-iodophenol (**12**) and *N*-benzyl-2-iodoaniline (**13**) did not undergo cyclisation under these conditions (**Scheme 4.12**).

Table 4.4. Substrate scope studies for the cyclisation of 2-iodo-*N*-allylanilines**Scheme 4.11.** Cyclisation attempt on *N*-cinnamoyl-2-iodoaniline**Scheme 4.12.** Cyclisation attempt on *O*-allyl-2-iodophenol (**12**) and *N*-benzyl-2-iodoaniline (**13**)

4.5.3. One pot sequential cyclisation attempt

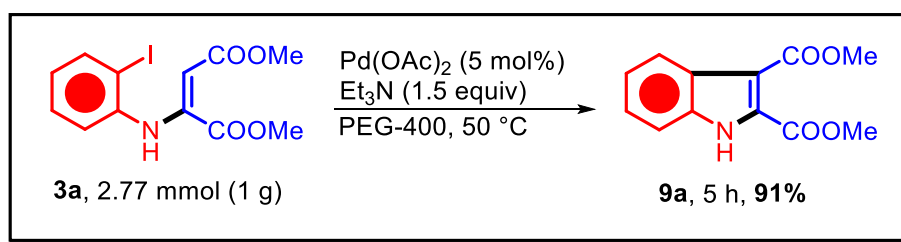
A one-pot sequential strategy was utilised for the generation of compound **9a**. Initially, 2-iodoaniline reacts with dimethyl/diethyl acetylenedicarboxylate (DMAD) in PEG-400, forming intermediate **4a** and **4b**. Subsequent treatment of the intermediate **4a** and **4b**. Subsequently, treatment of this intermediate with 5 mol% Pd(OAc)₂ and 1.5 equivalents of Et₃N facilitates the conversion to **9a** and **9b** in a streamlined, one-pot cascade process. However, the overall yields are comparatively lower than those obtained through the single-step transformation, as illustrated in **Scheme 4.13**.



Scheme 4.13. One pot sequential synthesis of **9a** and **9b**

4.5.4. Scale-up experiments

When scaled up to a 1-gram scale, the cyclisation of dimethyl 2-((2-iodophenyl)amino)maleate (**3a**) (**Scheme 4.14**) demonstrated excellent efficiency, yielding 0.5871 grams of the desired indole product **9a**. This corresponds to an impressive 91% yield achieved within a relatively short reaction time of 5 hours. The high yield and efficient reaction conditions highlight the robustness and practicality of this method for the synthesis of the indole product on a larger scale.



Scheme 4.14. Scaling the cyclisation of **3a** to gram scale

4.5.5. X-Ray crystallographic studies

Molecular structure of **9a** was obtained by using single crystal X-ray diffraction analysis. It reveals that **9a** crystallises in the tetragonal $R\bar{3}$ space group. Representative view of the molecular structure of **9a** is depicted in **Figure 4.1**. Relevant crystal data along with the refinement parameters are given in **Table 4.5**. As anticipated, the asymmetric unit of **9a** consists of functionalised indole where two carboxy ester groups are attached to *ortho* and *meta* positions respectively (C8 and C9).

Table 4.5. Crystallographic data for **9a**

Empirical formula	C ₁₂ H ₁₁ N ₁ O ₄	ρ_{calc} [Mg/m ³]	1.298
Formula weight	233.22	μ [mm ⁻¹]	0.099
Temperature/K	100 (2)	F(000)	504
Wavelength	0.71073 Å	Crystal size [mm³]	0.28 x 0.13 x 0.10
CCDC	2299474	Theta range for data collection	3.655 to 25.993°
Crystal system	Trigonal	Index ranges	-41 ≤ h ≤ 41, -41 ≤ k ≤ 41, -6 ≤ l ≤ 6
Space group	$R\bar{3}$	Reflections collected	51845
a/Å	33.45(2)	Independent reflections	2342 [R(int) = 0.2469]
b/Å	33.45(2)	Completeness to theta	99.8 %
		= 25.242°	

$c/\text{\AA}$	5.541(4)	Refinement method	Full-matrix least-squares on F^2
$\alpha/^\circ$	90	Data / restraints / parameters	2342 / 0 / 159
$\beta/^\circ$	90	Goodness-of-fit on F^2	1.071
$\gamma/^\circ$	120	Final R indices [$I > 2\sigma(I)$]	$R1 = 0.0781$, $wR2 = 0.2172$
Volume [\AA^3]	5369(7)	R indices (all data)	$R1 = 0.1260$, $wR2 = 0.2473$
Z	18		

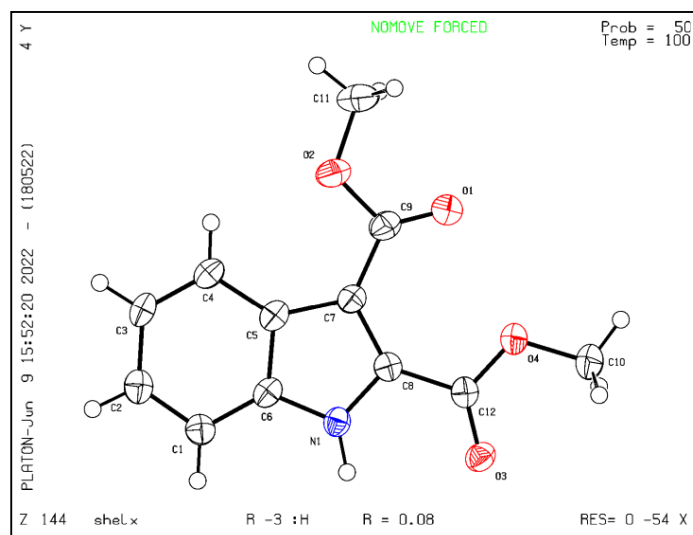


Figure 4.1. ORTEP diagram of **9a** with 50% probability ellipsoids

4.5.5.1. Hydrogen bonding pattern of **9a**

X-ray crystallographic studies further reveal that in **9a**, intermolecular hydrogen bonding occurs between the NH hydrogen atom (H11) and the carbonyl oxygen atom of the nearest neighboring unit (O3#1). This interaction ultimately results in the formation of a one-dimensional network through the establishment of a 10-membered ring (**Figure 4.2**). Further, **Table 4.6** shows some of the selected bond lengths and bond angles of **9a**.

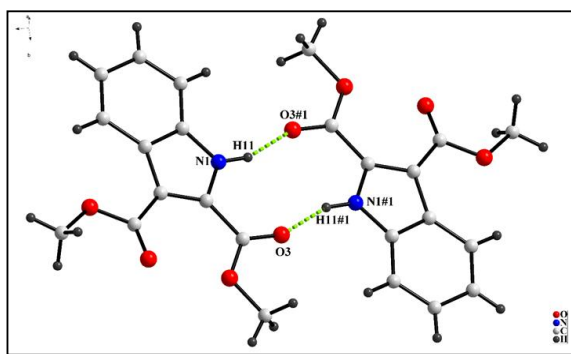


Figure 4.2. Hydrogen bonding pattern of **9a**

Table 4.6. Selected bond lengths and bond angles of **9a**

Bond Length [Å]			
O(1)-C(9)	1.182(5)	C(1)-C(6)	1.403(5)
O(2)-C(9)	1.350(4)	C(2)-C(3)	1.403(5)
O(2)-C(11)	1.443(5)	C(3)-C(4)	1.376(5)
O(3)-C(12)	1.212(4)	C(4)-C(5)	1.418(5)
O(4)-C(12)	1.324(4)	C(5)-C(6)	1.404(5)
O(4)-C(10)	1.440(5)	C(5)-C(7)	1.445(5)
N(1)-C(8)	1.364(5)	C(7)-C(8)	1.401(5)
N(1)-C(6)	1.372(4)	C(7)-C(9)	1.470(5)
C(1)-C(2)	1.372(5)	C(8)-C(12)	1.474(5)
Bond angles [°]			
C(9)-O(2)-C(11)	116.2(3)	O(1)-C(9)-C(7)	128.3(4)
C(12)-O(4)-C(10)	115.8(3)	O(1)-C(9)-O(2)	120.9(4)
C(8)-N(1)-C(6)	109.9(3)	O(3)-C(12)-C(8)	121.9(3)
C(2)-C(1)-C(6)	116.6(4)	O(3)-C(12)-O(4)	123.6(3)
C(1)-C(2)-C(3)	121.3(4)	O(4)-C(12)-C(8)	114.5(3)
C(4)-C(3)-C(2)	122.2(3)	N(1)-C(8)-C(7)	109.2(3)

4.5.6. Mechanistic studies

The classical Heck reaction, that usually involves the coupling of aryl halides with terminal/ internal alkenes to form substituted alkenes is catalysed by Pd(0). The use of palladium in the form of Pd(0) nanoparticles has immensely helped in the

escalation of the reaction rates of the Heck reaction [31]. The Pd(II)-PEG-400 reaction system utilised in this protocol is superior towards the reaction owing to the *in-situ* generation of Pd(0) nanoparticles. In case of the ligand free cyclisation of 2-iodo-N-vinylanilines, upon vigorous stirring Pd(II) with PEG-400, results in the reduction of Pd(II) to Pd(0) and formation of Pd(0) stabilised in the PEG-400 matrix. This catalytically active Pd(0) drives the reaction forward. PEG-400 is inexpensive, non-toxic and has tuneable properties. It has the capability of acting as both reducing agent as well as it prevents the agglomeration of nanoparticles [21, 28]. The *in-situ* generation of Pd(0) nanoparticles is evident from the TEM analysis (**Figure 4.3**). The particle size distribution pattern of the nanoparticles shows an average particle size of 8.52 nm (**Figure 4.4**).

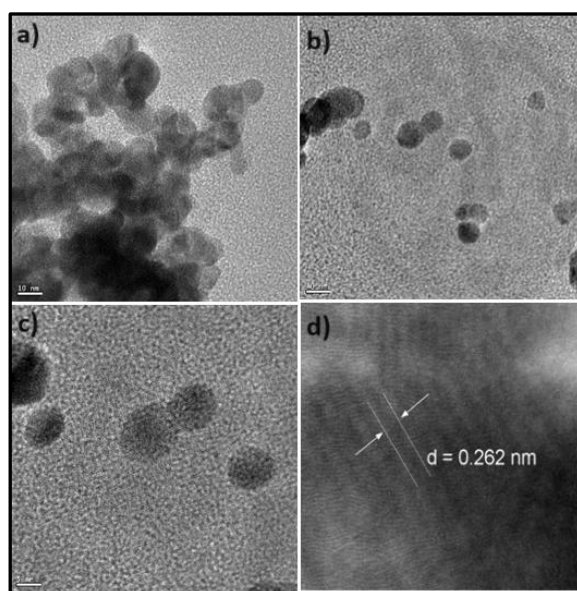


Figure 4.3 (a), (b), (c), (d). TEM images and *d*-spacing of the *in-situ* generated Pd nanoparticles

4.6. Reusability studies

The *in-situ* generated palladium nanoparticles obtained in the cyclisation of 3a can be reused for three consecutive cycles. The investigation into the reusability of the Pd(II)-PEG-400 system in the provided protocol was conducted using the optimised conditions outlined in **Scheme 4.10**. Results indicated that the catalytic system can undergo up to three consecutive cycles of reuse, albeit with some loss of activity observed in the cyclisation process (**Figure 4.5 (a)**).

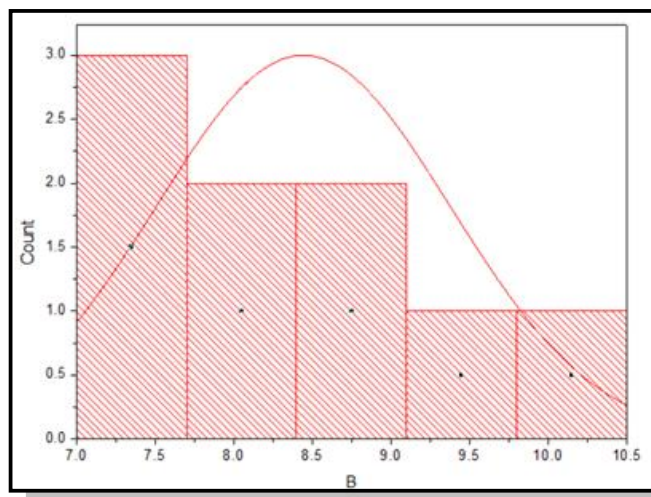


Figure 4.4. Particle size distribution histogram for the *in-situ* generated Pd nanoparticles

The system's reusability is ascribed to the heterogeneity of the *in-situ* formed Pd nanoparticles. Additionally, the decrease in catalytic activity may be attributed to the agglomeration of the nanoparticles. The system's heterogeneity is further confirmed by the hot filtration test, wherein the reaction ceases upon filtering the *in-situ* generated nanocatalyst from the reaction medium. The agglomeration of the nanoparticles is also evident from the TEM analysis (**Figure 4.5 (b, c)**).

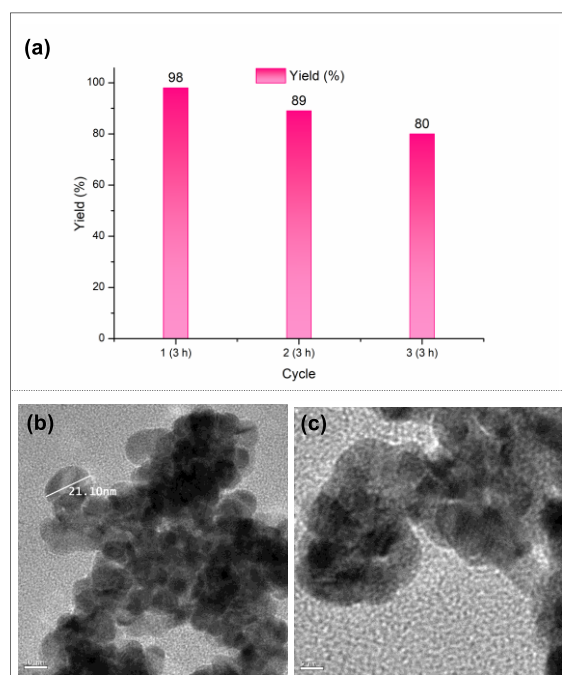
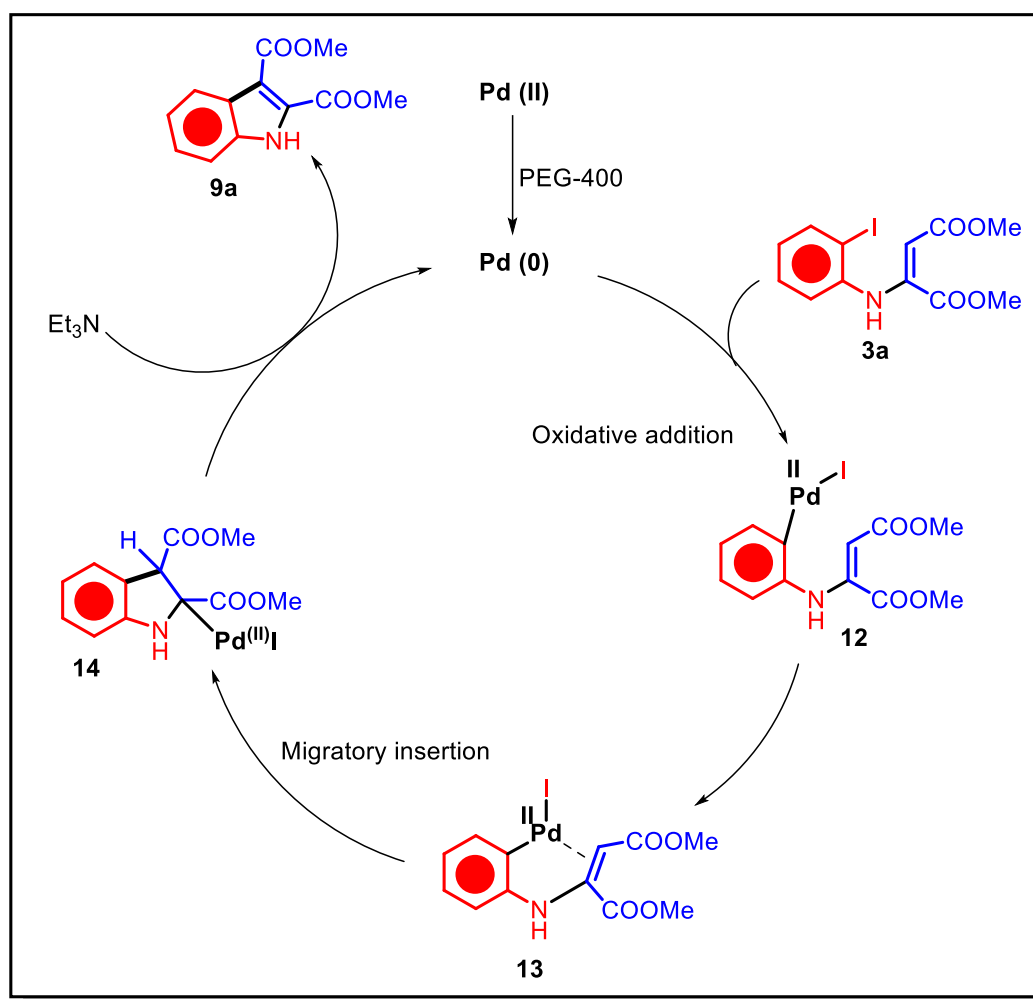


Figure 4.5. (a) Reusability profile of the reaction 3a to 4a; (b), (c) TEM images of the catalyst post 3rd cycle showing the agglomerated nanomaterial

4.7. Reaction mechanism

4.7.1. Cyclisation of *N*-vinyl-2-iodoanilines

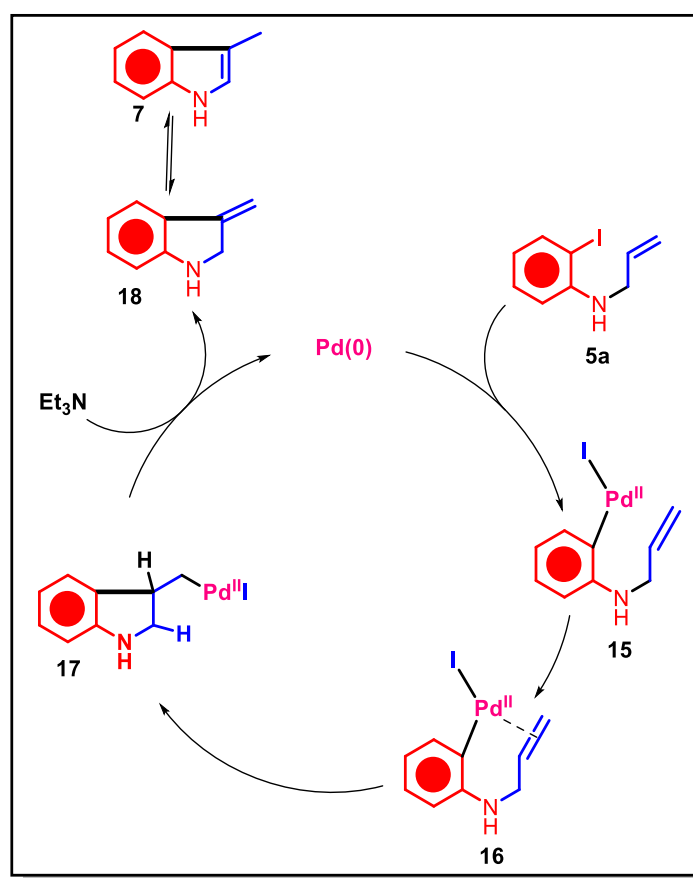
The described protocol represents an extension of the Heck reaction, which occurs between aryl halides and alkenes. In this method, the use of PEG-400 as the reaction medium, in conjunction with Pd(II), facilitates the *in-situ* formation of catalytically active Pd(0). A plausible mechanism, illustrated in **Scheme 4.15** begins with the addition of the C-halogen bond in *N*-vinyl-2-iodoaniline (**3a**) oxidatively to the Pd(0) center, resulting in the formation of the organopalladium (II) species (**12**). Subsequently, the Pd(II) center in species **12** undergoes intramolecular η^2 -ligation with the alkene, forming intermediate **13**. This intermediate then undergoes migratory insertion, followed by deprotonation, to yield the anticipated product (**9a**) and revive the Pd(0) catalyst, completing the catalytic cycle.



Scheme 4.15. Mechanism of Heck cyclisation of *N*-vinyl-2-iodoanilines

4.7.2. Cyclisation of *N*-allyl-2-iodoanilines

The cyclisation of *N*-allyl anilines proceeds *via* a mechanistically distinct pathway compared to their *N*-vinyl counterparts. Following the initial oxidative addition of the aryl halide moiety to the Pd(0) species, the resulting Pd(II) intermediate engages in η^3 -coordination with the allyl side chain of substrate **5a**. In this mode of coordination, the palladium center interacts simultaneously with all three carbon atoms of the allyl group, forming a stable π -allyl complex (**15**). This η^3 -binding is a key feature that stabilises the intermediate and correctly orients the reacting centers for the ensuing transformation. The geometry of this complex facilitates an intramolecular attack of the aryl ring on the electrophilic terminus of the allyl group *via* a migratory insertion step, thereby forming a new C–C bond. Subsequent deprotonation relieves the developing strain and helps rearomatise the ring, leading to cyclisation and formation of the 3-methylindole product (**10a**). The regeneration of Pd(0) at the end of the cycle completes the catalysis.



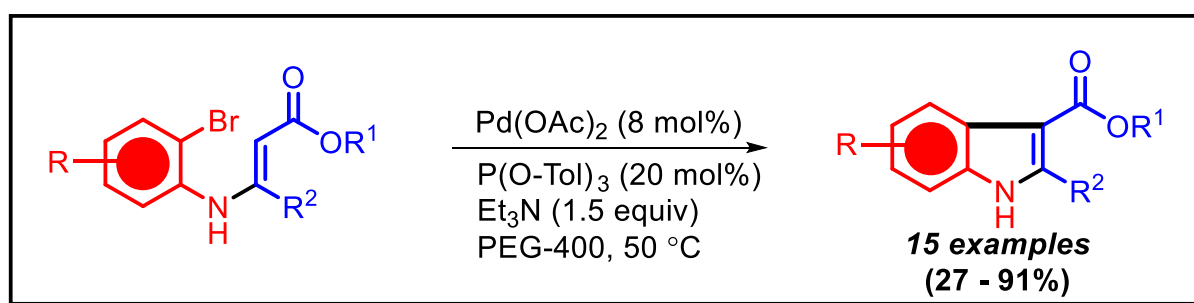
Scheme 4.16. Plausible mechanism for the cyclisation of *N*-allyl-2-iodoaniline for the generation of the 3-methylindole moiety

4.8. Conclusion

In conclusion, we demonstrated that under palladium catalysis, *N*-vinyl-2-iodo and *N*-allyl-2-iodo arenes undergo cyclisation under mild conditions, leading to the efficient formation of indole frameworks. These intermediates, synthesised *via* the Michael addition of 2-iodoanilines with propiolate esters, exhibit cyclisation potential, including their *N*-functionalised derivatives. The reactions are characterised by short durations and consistently high to excellent yields. This catalytic process owes its efficiency to the *in-situ* formation of palladium nanoparticles, with PEG-400 serving as both a reductant and a stabiliser. Furthermore, the system operates as a heterogeneous catalyst, maintaining its activity for up to three reuse cycles.

Chapter 4b

Palladium (II) – PEG System for the Efficient Synthesis of Indoles via Intramolecular Heck Cyclisation of *N*-vinyl-2-bromoarenes



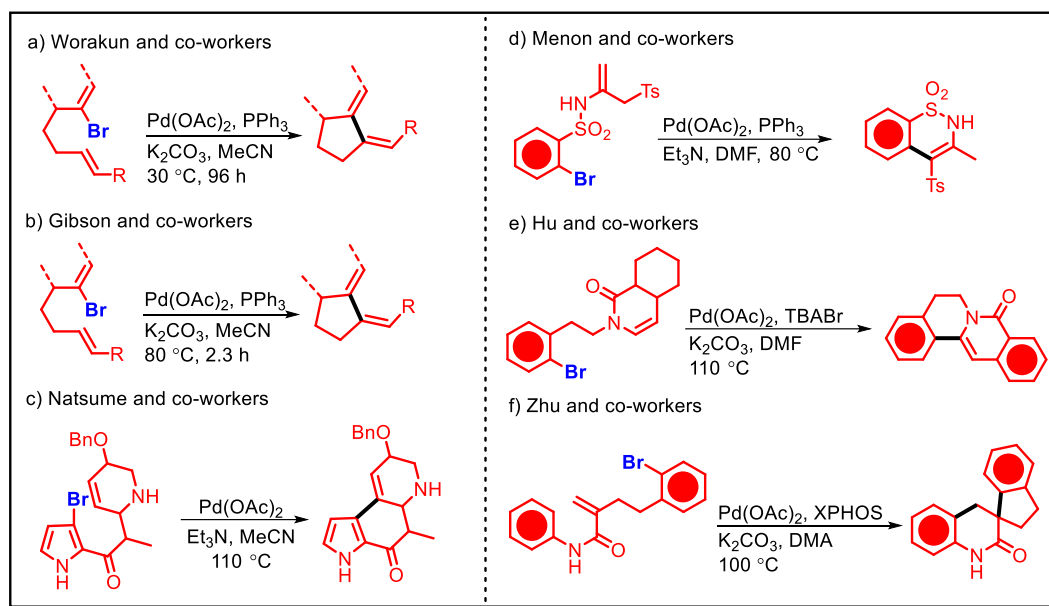
Abstract: The Palladium (II)-PEG system is used as a catalyst to efficiently promote the cyclisation of *N*-vinyl-2-bromoanilines. However, when applied to the cyclisation of 2-bromoaminoacrylate esters, the reaction required certain adjustments due to the higher bond energy of the aromatic sp² C-Br bond. These modifications involved increasing the catalyst loading, incorporating a σ -donor ligand and conducting the reaction at an elevated temperature, resulting in the successful production of substituted indoles.

Palladium (II) – PEG System for the Efficient Synthesis of Indoles *via* Intramolecular Heck Cyclisation of *N*-vinyl-2-bromoarenes

4.9. Introduction

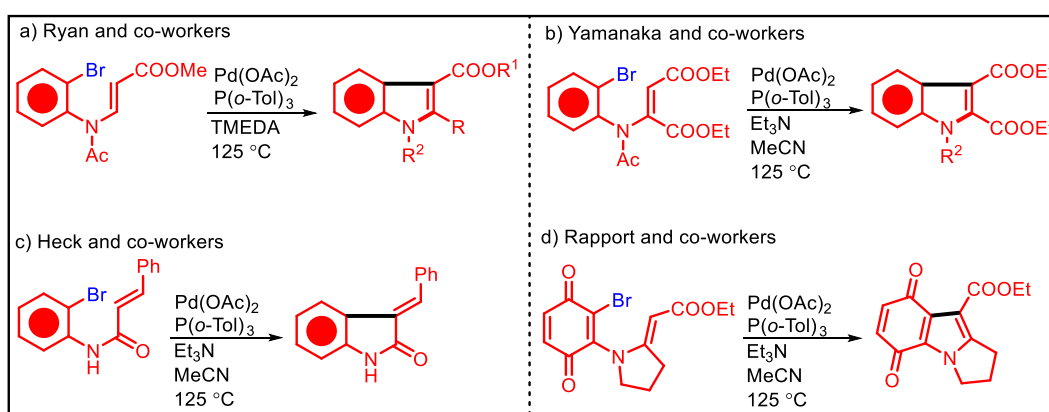
Carbon-carbon bond formation reactions involving cross-coupling tools, using aryl/vinyl bromides, include reactions such as Suzuki-Miyaura, Sonogashira, Kumada and Heck coupling reactions. With a bond dissociation energy that ranges from roughly 276 to 290 kJ/mol, the aryl C-Br bond is stronger than the aryl C-I bond (~238 kJ/mol) but weaker than the aryl C-Cl bond (~338 kJ/mol) [32]. Aryl bromides are excellent catalytic reaction substrates because of their intermediate bond strength, which strikes a compromise between stability and reactivity. A low-valent metal catalyst, like Pd(0) or Ni(0), reacts with the aryl C-Br bond during oxidative addition, a crucial stage in many transition metal-catalysed reactions. Strong σ -donor ligands, like phosphines or *N*-heterocyclic carbenes (NHCs), are frequently necessary for this reaction to occur. By increasing the electron density on the metal centre, these ligands reduce the activation energy needed for oxidative addition, which makes it easier to cleave the sp^2 C-Br bond [33]. Furthermore, to ensure catalytic performance, σ -donor ligands stabilise the metal complex's higher oxidation state, which is usually Pd(II) or Ni(II) [20]. Aryl bromides are perfect for coupling reactions like Suzuki-Miyaura, Heck, and Negishi because of their moderate bond energy and the electron-donating properties of these ligands, which enable effective activation in mild circumstances. Because of these characteristics, aryl bromides are essential for the synthesis of a wide range of chemical compounds.

Aryl bromides have proven to be highly effective in the creation bonds between carbons by the Heck reaction. This method has significantly contributed to the synthesis of various carbocycles, as demonstrated in studies conducted by researchers like the Worakun [34], Tozer [35], and Natsube [36] groups. Additionally, aryl bromides have been instrumental in the synthesis of heterocycles, with notable contributions from the research groups such as Menon [37], Hu [38], and Zhu [39]. (Scheme 4.17).



Scheme 4.17. Synthesis of carbocycles and heterocycles *via* intramolecular Heck cyclisation involving aryl/vinyl bromides

Aryl bromide bearing moieties have also been successfully cyclised under Heck conditions to produce five membered heterocycles that includes indoles [30]. The cyclisation, however requires the use of phosphorous ligands for effective transformation and have been studied by research groups such as Ryan [40], Yamanaka [29], Heck [41] and Rapport [42] (**Scheme 4.18**).



Scheme 4.18. Synthesis of indole systems *via* intramolecular Heck cyclisation involving aryl bromides

Herein, we utilise the Palladium (II) - PEG system as a catalyst to efficiently promote the cyclisation of *N*-vinyl-2-bromoanilines. However, for the cyclisation of 2-bromoaminoacrylate esters, modifications were necessary due to the higher bond

energy of the aromatic sp^2 C-Br bond. These adjustments involved increasing the catalyst loading, introducing a σ -donor ligand, and conducting the reaction at elevated temperatures, ultimately achieving the successful synthesis of substituted indoles.

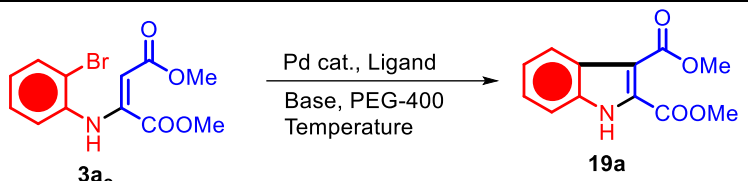
4.10. Optimisation of reaction conditions for the cyclisation of 2-bromo-*N*-vinylanilines

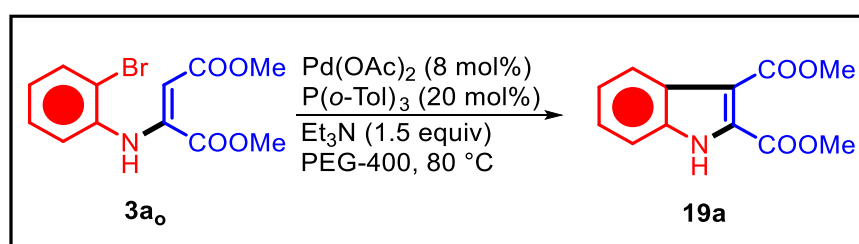
The cyclisation of dimethyl-2-((2-bromophenyl)amino)maleate (**3a_o**) was chosen as the model reaction to optimise reaction conditions, with the results summarised in **Table 4.4**. Firstly, the reaction was conducted using 5 mol% of Pd(OAc)₂, 2 equivalents of Et₃N, and PEG-400 as the reaction medium at 50 °C, based on the optimised conditions outlined in **Scheme 4.10**. This setup yielded only trace amounts of the product (**19a**) after 6 hours (**Entry 1**). Increasing the catalyst loading to 8 mol% and raising the temperature to 60 °C, while keeping other conditions constant, improved the yield to 23% (**Entry 2**). Significant improvement was observed when a σ -donor ligand, P(*o*-Tol)₃, was introduced at 20 mol%. In the presence of 5 mol% of the Pd(II) catalyst, 1.5 equivalents of Et₃N, and a reaction temperature of 90 °C, the product yield increased dramatically to 89% within 3.5 hours (**Entry 3**). Further optimisation using 8 mol% of Pd(OAc)₂ and 20 mol% of the ligand at 80 °C increased the yield slightly to 91% (**Entry 4**). However, substituting Et₃N with 1.5 equivalents of K₂CO₃ under these conditions resulted in no product formation (**Entry 5**). The use of 5 mol% of PdCl₂ instead of Pd(OAc)₂ led to a significant decrease in yield to 27% at 60 °C (**Entry 6**). Reducing the Pd(OAc)₂ loading to 2 mol% also lowered the yield, achieving 59% with 1.5 equivalents of Et₃N and 62% with 2 equivalents of Et₃N (**Entries 7 and 8**). Using 5 mol% of Pd(PPh₃)₄ resulted in reduced yields of 72% and 70% in the presence and absence of P(*o*-Tol)₃, respectively (**Entries 9 and 10**). These results highlight the critical role of catalyst choice, ligand, base, and reaction parameters in achieving optimal yields.

The optimised reaction condition can therefore be summarised as: **3a_o** (1 equiv), Pd(OAc)₂ (8 mol%), P(*o*-Tol)₃ (20 mol%), Et₃N (1.5 equiv), PEG-400, 80 °C (**Scheme 4.19**). The higher temperature, along with the presence of a σ -donor ligand such as tris-*ortho*-tolylphosphine (P(*o*-Tol)₃), facilitates a better oxidative addition of the

stronger, kinetically less labile sp^2 -C-Br bond to the Pd(0) centers, thereby ensuring effective conversion.

Table 4.7. Optimisation of the reaction conditions for the cyclisation of **3a_o** to **19a**.

							
Sl.	Catalyst (mol%)	Ligand (20 mol%)	Base (eq.)	Solvent	Temp.	Time	Yield
1	Pd(OAc) ₂ (5)		Et ₃ N (2)	PEG-400	50 °C	6 h	Trace
2	Pd(OAc) ₂ (8)		Et ₃ N (2)	PEG-400	60 °C	6 h	23%
3	Pd(OAc) ₂ (5)	P(o-Tol) ₃	Et ₃ N (1.5)	PEG-400	90 °C	3.5 h	89%
4	Pd(OAc)₂ (8)	P(o-Tol)₃	Et₃N (1.5)	PEG-400	80 °C	3.5 h	91%
5	Pd(OAc) ₂ (8)	P(o-Tol) ₃	K ₂ CO ₃ (1.5)	PEG-400	80 °C	4 h	NR
6	PdCl ₂ (5)	P(o-Tol) ₃	Et ₃ N (1.5)	PEG-400	60 °C	4 h	27%
7	Pd(OAc) ₂ (2)	P(o-Tol) ₃	Et ₃ N (1.5)	PEG-400	80 °C	6 h	59% ^a
8	Pd(OAc) ₂ (2)	P(o-Tol) ₃	Et ₃ N (2)	PEG-400	80 °C	6 h	62% ^a
9	Pd(PPh ₃) ₄ (5)		Et ₃ N (1.5)	PEG-400	80 °C	6 h	72%
10	Pd(PPh ₃) ₄ (5)	P(o-Tol) ₃	Et ₃ N (1.5)	PEG-400	80 °C	6 h	70%
Reaction conditions: 3a_o (1 eq., 0.2 mmol), Pd(OAc) ₂ (5 mol%), PEG (1 mL)							

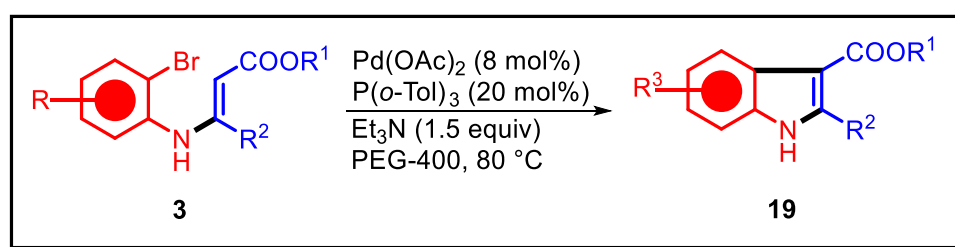


Scheme 4.19. Optimised reaction condition for the cyclisation of **3a_o** to **19a**

4.11. Substrate scope studies

4.11.1. General procedure for the cyclisation of *N*-vinyl-2-bromoanilines

A thoroughly cleaned and dried sealed tube (VENSIL™) was prepared and charged with the following components: 1 equivalent (0.1 mmol) of 2-((2-bromophenyl)amino)maleates, 8 mol% palladium acetate as the catalyst, 20 mol% tri-*o*-tolyl phosphine as the ligand, and 1.5 equivalents of triethylamine as the base, dissolved in 1.5 mL of PEG-400 as the solvent. The reaction mixture was stirred at 80 °C for 3.5 hours, with progress monitored by thin-layer chromatography (TLC). Upon completion, the reaction was quenched by adding saturated ammonium chloride solution. The mixture was then filtered through a celite plug and extracted three times with ethyl acetate (3 × 20 mL). The combined organic layers were washed with brine, dried over anhydrous sodium sulfate, and concentrated under reduced pressure to obtain the crude product. The crude product was purified using silica gel column chromatography (60–120 mesh silica gel) with a gradient elution of 10%–20% ethyl acetate in hexanes. This process yielded the pure indole products (**Scheme 4.20**).



Scheme 4.20. Cyclisation of *N*-vinyl-2-bromoanilines

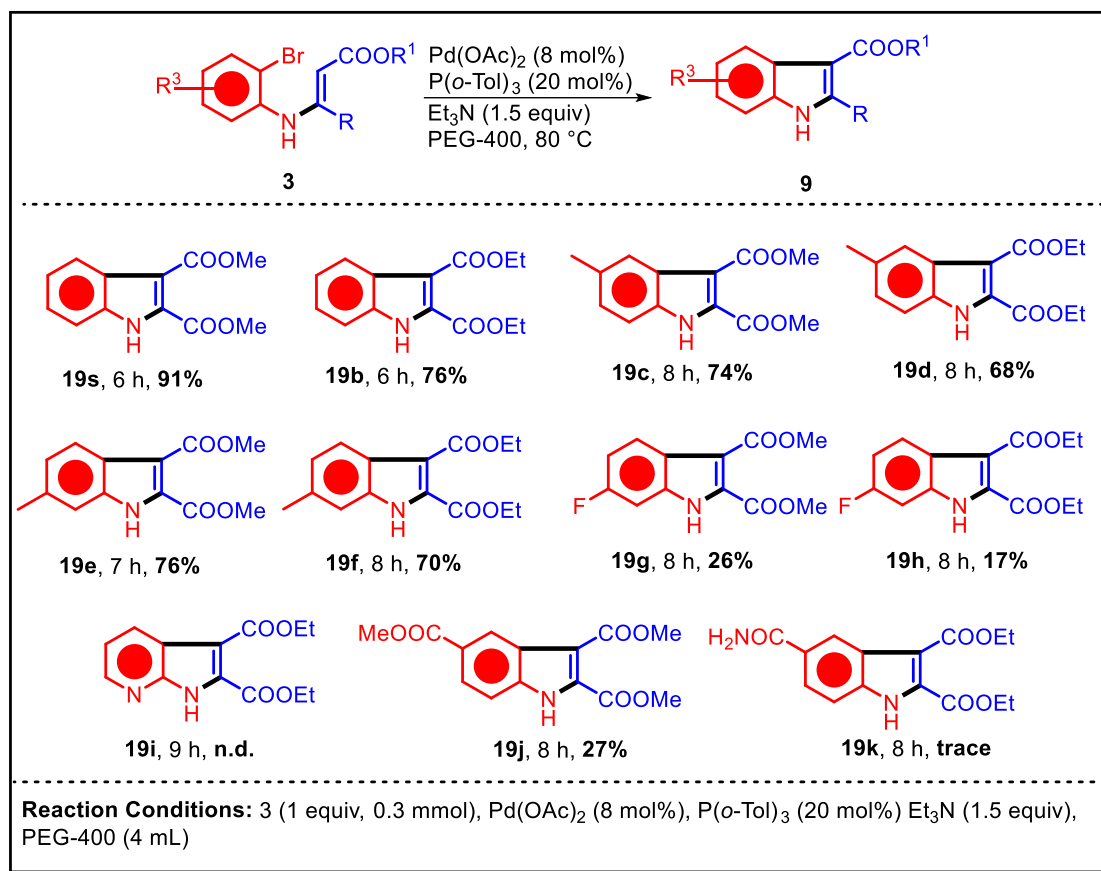
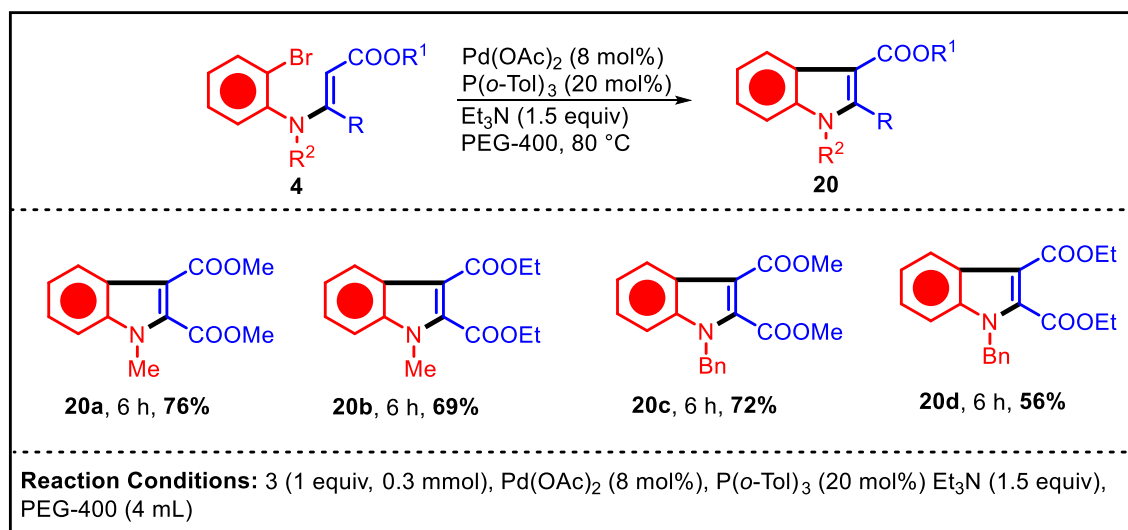
4.11.2. Substrate scope for the cyclisation of *N*-vinyl-2-bromoanilines

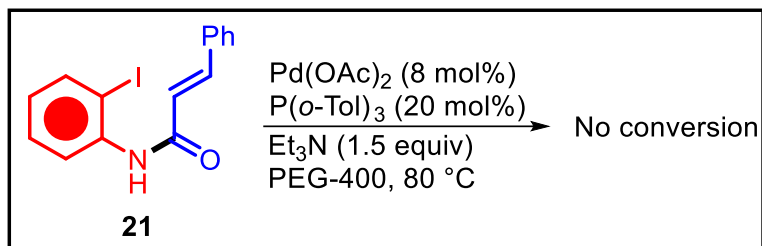
After optimising the reaction, we went on to explore the reaction scope using a variety of electronically diverse substrates. The results are summarised in **Table 4.8**. The cyclisation of the adduct **3a**, derived from 2-bromoaniline and DMAD, produced the indole **19a** with an excellent yield of 91% in 6 hours. Similarly, the cyclisation of **3b**, formed from 2-bromoaniline and DEAD, afforded the indole **19b** with a 76% yield in 6 hours. When the substrates **3c** and **3d**, derived from 4-methyl-2-bromoaniline with DMAD and DEAD respectively, were cyclised, the resulting indoles **19c** and **19d** were obtained in yields of 74% and 68%, respectively, over 8 hours. The cyclisation of the adducts **3e** and **3f**, derived from 5-methyl-2-bromoaniline with DMAD and DEAD,

gave indoles **19e** and **19f** with yields of 76% and 70%, achieved in 7 and 8 hours, respectively. In contrast, the cyclisation of adducts **3go** and **3ho**, derived from 5-methyl-2-bromoaniline with DMAD and DEAD, resulted in significantly lower yields of indoles **19g** and **19h**, which were only 26% and 17%, respectively, after 8 hours. Furthermore, the adduct **3io**, containing a pyridine nucleus, did not produce the anticipated product **19i** underneath the same settings. Adducts containing electron-withdrawing groups, like esters and amides, namely **3jo** and **3ko**, demonstrated sluggish reactivity. Their cyclisation resulted in poor yields of the desired indoles **19j** and **19k**, highlighting the sensitivity of the reaction to electronic effects.

This was followed by studying the scope of the reaction with *N*-alkylated and benzylated adducts. The cyclisation of *N*-methylated adduct (**4ao**) of **3ao** yielded 76% of the product **20a**. The cyclisation of *N*-methylated adduct (**4bo**) of **3bo** yielded 69% of the product **20a** in 6 hours. Subsequently the cyclisation of the *N*-benzylated adducts **4co** and **4do** of **3co** and **3do** yielded 72% and 56% of the products **20c** and **20d** respectively in 6 hours (**Table 4.9**).

Additionally, the cyclisation attempt on *N*-cinnamoyl-2-bromoaniline did not give any desired result (**Scheme 4.21**)

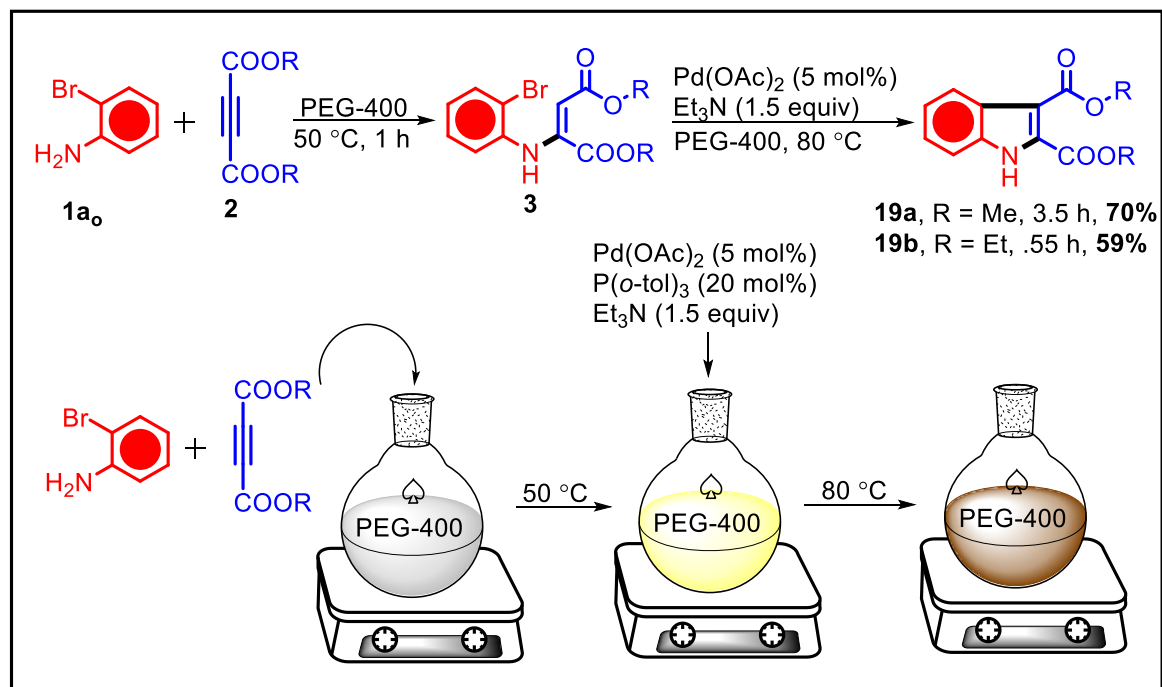
Table 4.8. Substrate scope for the cyclisation of *N*-vinyl-2-iodoanilines**Table 4.9.** Substrate scope for the cyclisation of *N*-alkyl and benzyl adducts



Scheme 4.21. Cyclisation attempt on *N*-cinnamoyl-2-bromoaniline

4.11.3. One pot sequential cyclisation attempt

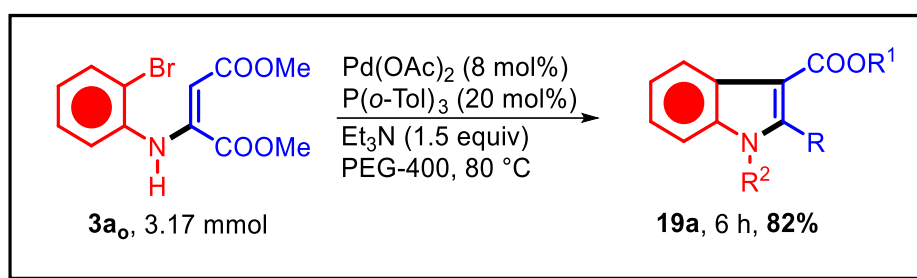
A one-pot sequential strategy was employed for the synthesis of compounds **19a** and **19b**. Initially, 2-iodoaniline reacts with dimethyl or diethyl acetylenedicarboxylate (DMAD) in PEG-400, resulting in the in-situ formation of intermediates **4a_o** and **4b_o**. These intermediates are then treated with 5 mol% Pd(OAc)₂ and 1.5 equivalents of Et₃N, enabling their conversion into **19a** and **19b** via a streamlined, one-pot cascade process, akin to the cyclisation of the iodo analogue. However, the overall yields from this approach are relatively lower compared to those obtained through the single-step transformation, as illustrated in **Scheme 4.22**.



Scheme 4.22. One pot cyclisation to form **19a**

4.11.4. Scale-up experiments

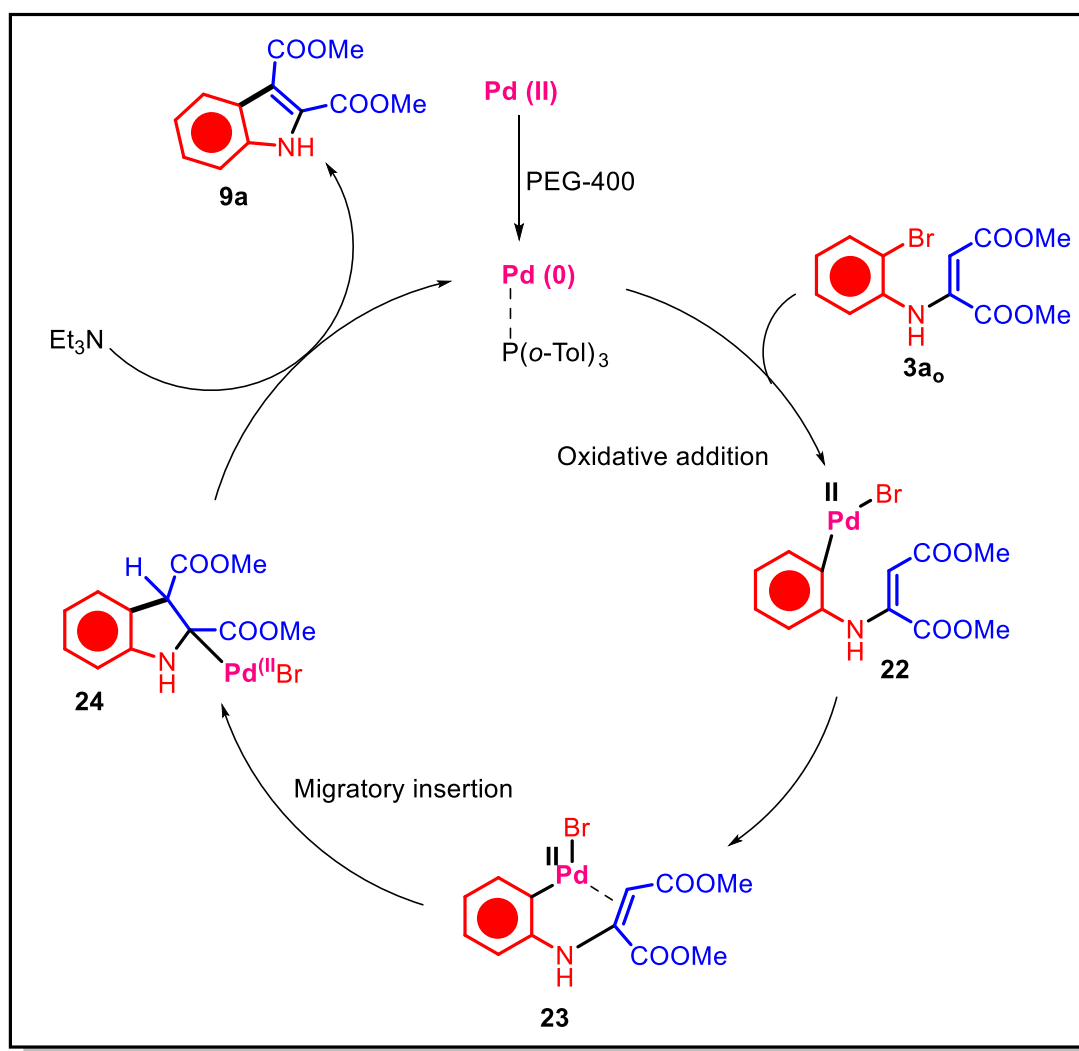
When scaled up to a 1-gram scale, the cyclisation of dimethyl 2-((2-bromophenyl)amino)maleate (**3a_o**) (**Scheme 4.23**) demonstrated good efficiency. The reaction yielded the desired indole product **19a**, corresponding to an impressive 82% yield within a short reaction time of just 6 hours. These results underscore the high yield, efficient reaction conditions, and the overall robustness and practicality of this method for large-scale synthesis of the indole product.



Scheme 4.23. Scaling the cyclisation of **3a_o** to gram scale

4.11.5. Reaction mechanism

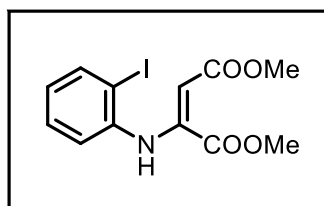
A likely mechanism, illustrated in **Scheme 4.24**, initiates with the oxidative addition of the carbon halogen bond in N-vinyl-2-bromoaniline (**3a_o**) to the Pd(0) center. This Pd(0) species is formed in the presence of PEG-400 and is coordinated with a phosphine ligand. This step results in the formation of the organopalladium (II) species (**22**). Next, the Pd(II) center in species **22** undergoes intramolecular η^2 -ligation with the alkene, forming the intermediate **23**. Subsequently, this intermediate undergoes migratory insertion, followed by a deprotonation step, to afford the desired product (**19a**) while regenerating the Pd(0) catalyst, thus completing the catalytic cycle.



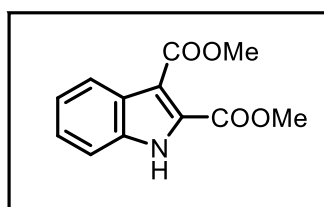
Scheme 4.24. Reaction mechanism for the Pd catalysed cyclisation of **3a_o** to **19a**

4.12. Conclusion

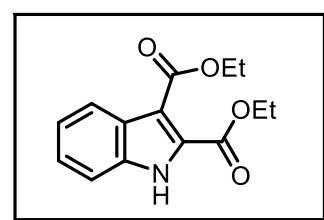
In conclusion, we have successfully shown that *N*-vinyl-2-bromoanilines undergo efficient cyclisation under palladium catalysis, resulting in the formation of indole frameworks under mild conditions. These intermediates, synthesised *via* the Michael addition of 2-iodoanilines with propiolate esters, display excellent cyclisation potential, including for their *N*-functionalised derivatives. However, the use of a σ -donor ligand is essential to facilitate the oxidative addition of the kinetically less reactive C-Br bond. The reactions are characterised by short durations and consistently high to excellent yields, highlighting the efficiency and practicality of this catalytic system for indole synthesis.

4.13. ^1H and ^{13}C NMR Data

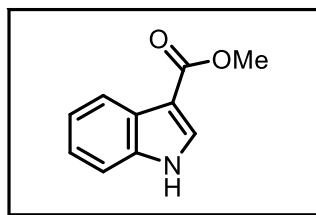
1. 3a. Dimethyl 2-((2-iodophenyl)amino)maleate, yellow oily liquid: ^1H NMR (400 MHz, CHLOROFORM- D_3) 9.62 (s, 1H), 7.80 (d, $J = 8.0$ Hz, 1H), 7.21 (t, $J = 7.7$ Hz, 1H), 6.79 (t, $J = 7.7$ Hz, 1H), 6.73 (d, $J = 8.0$ Hz, 1H), 3.75 (s, 3H), 3.66 (s, 3H). ^{13}C NMR (100 MHz, CHLOROFORM- D_3) δ 164.6, 161.4, 134.8, 128.1, 126.9, 126.0, 122.8, 122.7, 112.0, 52.8, 52.0



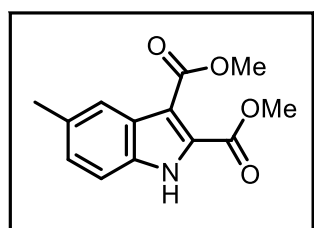
2. 9a. Dimethyl 1H-indole-2,3-dicarboxylate, white crystalline solid: ^1H NMR (400 MHz, CHLOROFORM- D_3) δ (ppm) 9.33 (s, 1H), 8.05 (d, $J = 8.2$ Hz, 1H), 7.43 (d, $J = 8.2$ Hz, 1H), 7.39 - 7.34 (m, 1 H), 7.30 - 7.26 (m, 1H), 3.98 (s, 3H), 3.98 (s, 3H). ^{13}C NMR (100 MHz, CHLOROFORM- D_3) δ 169.6, 164.4, 146.8, 141.8, 139.5, 128.8, 125.6, 120.8, 120.7, 95.9, 91.9, 52.9.



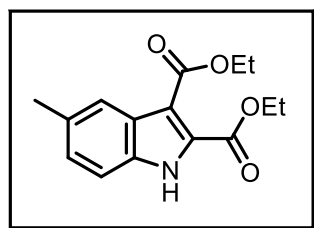
3. 9b. Diethyl 1H-indole-2,3-dicarboxylate, colourless oil: ^1H NMR (500 MHz, CHLOROFORM- D_3) δ (ppm) 9.34 (s, 1H), 8.05 (d, $J = 8.2$ Hz, 1H), 7.43 (d, $J = 8.2$ Hz, 1H), 7.36 (s, 1H), 7.29 - 7.24 (m, 1H), 4.45 (m, 4H), 1.43 (m, 6H). ^{13}C NMR (125 MHz, CHLOROFORM- D_3) 164.3, 161.0, 134.8, 128.2, 126.9, 125.8, 122.7, 122.4, 112.3, 111.9, 61.9, 60.8, 14.4, 14.2.



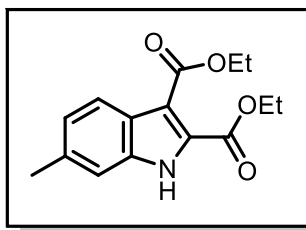
4. 9c. Methyl 1*H*-indole-3-carboxylate, white solid: ^1H NMR (600 MHz, CHLOROFORM- D_3) δ (ppm) 8.79 (s, 1H), 8.22 (d, $J = 6.0$ Hz, 1H), 7.95 (s, 1H), 7.45 (d, $J = 7.3$ Hz, 1H), 7.33 – 7.27 (m, 2H), 3.96 (s, 3H). ^{13}C NMR (150 MHz, CHLOROFORM- D_3) δ (ppm) 165.8, 136.1, 131.1, 125.8, 123.2, 122.1, 121.6, 111.6, 108.8, 81.1.



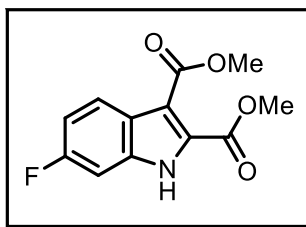
5. 9d, Dimethyl 5-methyl-1*H*-indole-2,3-dicarboxylate, white solid: ^1H NMR (600 MHz, CHLOROFORM- D_3) δ (ppm) 9.35 (s, 1H), 7.86 (s, 1H), 7.35 (d, $J = 8.4$ Hz, 1H), 7.22 (d, $J = 8.4$ Hz, 1H), 4.02 (s, 3H), 4.00 (s, 3H), 2.50 (s, 3H). ^{13}C NMR (150 MHz, CHLOROFORM- D_3) δ (ppm) 164.8, 161.4, 133.2, 132.2, 127.9, 127.9, 127.1, 121.9, 111.6, 111.4, 52.7, 51.8, 21.6.



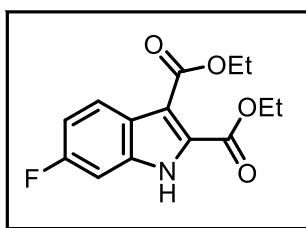
6. 9e, Diethyl 5-methyl-1*H*-indole-2,3-dicarboxylate, colourless oil: ^1H NMR (600 MHz, CHLOROFORM- D_3) δ (ppm) 9.23 (s, 1H), 7.86 (s, 1H), 7.35 (d, $J = 8.4$ Hz, 1H), 7.22 (d, $J = 8.4$ Hz, 1H), 4.52 – 4.44 (m, 4H), 2.50 (s, 3H), 1.5 – 1.43 (m, 6H). ^{13}C NMR (150 MHz, CHLOROFORM- D_3) δ (ppm) 164.5, 161.0, 133.2, 132.1, 128.0, 127.8, 127.2, 121.8, 111.7, 111.5, 61.8, 60.7, 21.7, 14.4, 14.3.



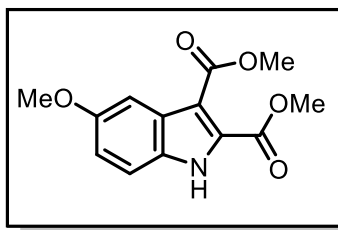
7. 9g, Diethyl 6-methyl-1H-indole-2,3-dicarboxylate, colourless oil: ^1H NMR (600 MHz, CHLOROFORM-D) δ (ppm) 9.24 (s, 1H), 7.94 (d, $J = 8.4$ Hz, 1H), 7.23 (s, 1H), 7.12 (d, $J = 8.4$ Hz, 1H), 4.53 – 4.41 (m, 4H), 2.50 (s, 3H), 1.48 - 1.44 (m, 6H). ^{13}C NMR (150 MHz, CHLOROFORM-D) δ 164.4, 161.1, 136.1, 135.2, 127.4, 124.9, 124.6, 122.2, 112.3, 112.3, 111.4, 61.7, 60.7, 21.9, 14.4, 14.2.



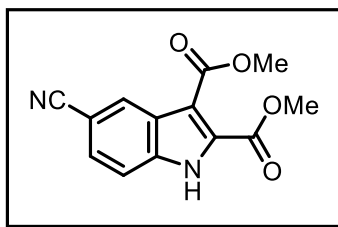
8. 9j, Dimethyl 6-fluoro-1H-indole-2,3-dicarboxylate, pale yellow solid: ^1H NMR (600 MHz, DMSO-D₆) δ (ppm) 12.69 (s, 1H), 7.92 (dd, $J = 9.0, 5.4$ Hz, 1H), 7.26 (dd, $J = 9.4, 2.0$ Hz, 1H), 7.13 (td, $J = 9.4, 2.3$ Hz, 1H), 3.91 (s, 3H), 3.86 (s, 3H). ^{13}C NMR (150 MHz, DMSO-D₆) δ 164.2, 161.7, 160.9 (d, $J = 262$ Hz), 135.7, 130.8, 123.6, 122.9, 111.7, 110.0, 98.9, 53.1, 52.1.



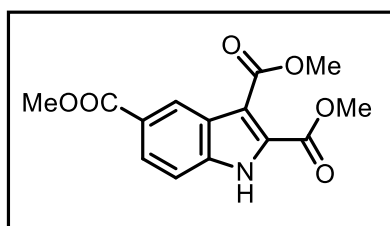
9. 9k, Diethyl 6-fluoro-1H-indole-2,3-dicarboxylate, white solid: ^1H NMR (600 MHz, CHLOROFORM-D) δ (ppm) 9.63 (s, 1H), 8.01 (dd, $J = 8.9, 5.3$ Hz, 1H), 7.13 (dd, $J = 9.0, 1.9$ Hz, 1H), 7.07 – 7.01 (m, 1H), 4.48 (q, $J = 3.3$ Hz, 4H), 4.47 (q, $J = 3.3$ Hz, 4H), 1.46 (t, $J = 6$ Hz, 3H), 1.45 – 1.41 (t, $J = 6$ Hz, 3H). ^{13}C NMR (150 MHz, CDCl₃) δ 164.0, 162.5, 160.9 (d, $J = 262$ Hz), 135.0, 128.6, 124.1, 123.5, 112.4, 111.9, 97.9, 62.0, 60.9, 14.4, 14.2.



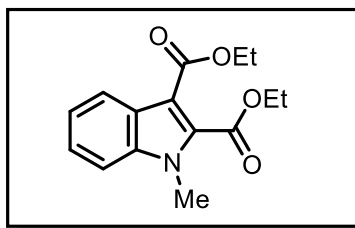
10. 9m, Dimethyl 5-methoxy-1H-indole-2,3-dicarboxylate, white solid: ^1H NMR (400 MHz, CHLOROFORM-D) δ (ppm) 9.25 (s, 1H), 7.47 (d, J = 2.5 Hz, 1H), 7.31 (d, J = 9.0 Hz, 1H), 7.02 (dd, J = 9.0, 2.5 Hz, 1H), 3.97 (s, 3H), 3.96 (s, 3H), 3.87 (s, 3H). ^{13}C NMR (100 MHz, CHLOROFORM-D) δ 164.9, 161.3, 156.2, 130.0, 128.2, 127.9, 117.9, 112.9, 111.3, 102.6, 55.7, 52.7, 51.9.



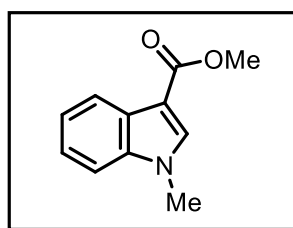
11. 9n, Dimethyl 5-cyano-1H-indole-2,3-dicarboxylate, white solid: ^1H NMR (400 MHz, CHLOROFORM-D) δ (ppm) 9.86 (s, 1H), 8.15 (d, J = 8.6 Hz, 1H), 7.82 (m, 1H), 7.47 (dd, J = 8.5, 1.5 Hz, 1H), 4.00 (s, 3H), 3.99 (s, 3H). ^{13}C NMR (100 MHz, CHLOROFORM-D) δ 163.8, 160.9, 133.5, 131.6, 129.6, 125.0, 124.1, 119.4, 117.2, 112.0, 108.7, 53.3, 52.3. Elemental Analysis (Observed) %N (10.47%), %C (60.22%), %H (3.94%), %O (25.37%).



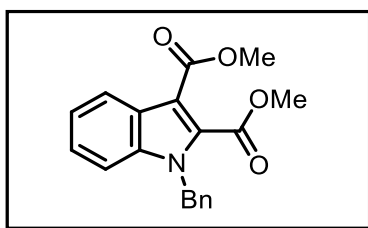
12. 9p, Trimethyl 1H-indole-2,3,5-tricarboxylate, white solid: ^1H NMR (400 MHz, CHLOROFORM-D) δ (ppm) 9.69 (s, 1H), 8.21 (dd, J = 1.6, 0.9 Hz, 1H), 8.14 – 8.05 (m, 1H), 7.91 (dd, J = 8.8, 1.7 Hz, 1H), 3.99 (s, 3H), 3.98 (s, 3H), 3.95 (s, 3H). ^{13}C NMR (100 MHz, CHLOROFORM-D) δ 167.3, 164.2, 161.1, 134.1, 131.0, 130.1, 127.6, 123.2, 122.7, 114.5, 111.8, 53.1, 52.4, 52.1.



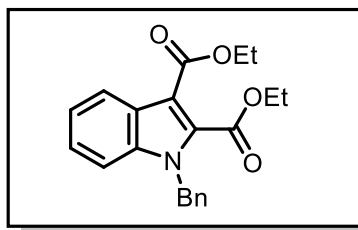
13. 9s, Diethyl 1-methyl-1H-indole-2,3-dicarboxylate, yellow oil: ^1H NMR (600 MHz, CHLOROFORM-D) δ (ppm) 8.17 (d, J = 8 Hz, 1H), 7.38 (m, 2H), 7.35 – 7.29 (m, 1H), 4.51 (q, J = 7.1 Hz, 2H), 4.42 (q, J = 7.1 Hz, 2H), 3.9 (s, 3H), 1.50 – 1.40 (m, 6H) ^{13}C NMR (151 MHz, CHLOROFORM-D) δ 164.2, 162.9, 136.8, 135.0, 125.4, 124.4, 122.5, 122.4, 110.1, 108.0, 62.3, 60.2, 31.4, 14.4, 14.1.



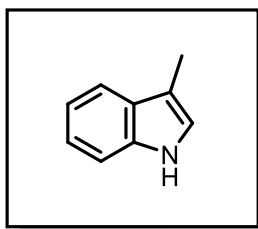
14. 9t, Methyl 1-methyl-1H-indole-3-carboxylate, colourless oil: ^1H NMR (600 MHz, CHLOROFORM-D) δ (ppm) 8.26 – 8.17 (m, 1H), 7.79 (s, 1H), 7.40 – 7.27 (m, 3H), 3.94 (s, 3H), 3.83 (s, 3H). ^{13}C NMR (150 MHz, CHLOROFORM-D) δ 165.5, 137.2, 135.2, 126.6, 122.8, 121.9, 121.6, 109.8, 106.9, 51.0, 33.4.



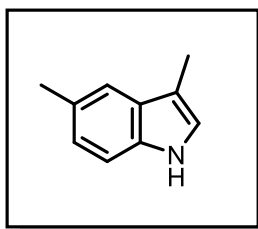
15. 9u, Dimethyl 1-benzyl-1H-indole-2,3-dicarboxylate, colourless oil: ^1H NMR (600 MHz, CHLOROFORM-D) δ (ppm) 8.19 - 8.16 (1H), 7.37 – 7.25 (m, 6H), 7.13 (d, J = 7.3 Hz, 2H), 5.49 (s, 2H), 3.97 (s, 3H), 3.93 (s, 3H). ^{13}C NMR (150 MHz, CHLOROFORM-D) δ 164.5, 163.3, 136.5, 136.1, 134.6, 128.8, 127.9, 126.6, 125.4, 124.7, 122.8, 122.4, 110.8, 108.6, 53.0, 51.6, 48.5.



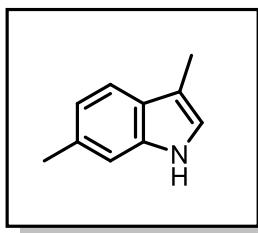
16. 9v, Diethyl 1-benzyl-1H-indole-2,3-dicarboxylate, yellow oil: ^1H NMR (600 MHz, CHLOROFORM-D) δ (ppm) 7.38 – 7.24 (m, 7H), 7.14 (d, J = 7.1 Hz, 2H), 5.49 (s, 2H), 4.43 (q, J = 7.1 Hz, 2H), 4.39 (q, J = 7.1 Hz, 2H), 1.44 (t, J = 7.1 Hz, 3H), 1.30 (t, J = 7.1 Hz, 3H). ^{13}C NMR (150 MHz, CHLOROFORM-D) δ (ppm) 164.1, 162.9, 136.5, 136.2, 135.0, 128.8, 127.9, 126.7, 125.6, 124.6, 122.7, 122.4, 110.7, 108.5, 62.3, 60.3, 48.5, 14.4, 13.9.



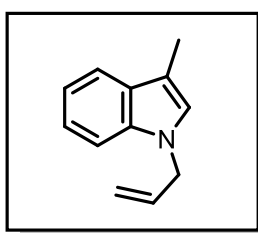
17. 10a, 3-Methyl-1H-indole, white crystalline solid: ^1H NMR (600 MHz, CHLOROFORM-D) δ (ppm) 7.91 (s, 1H), 7.63 (d, J = 7.8 Hz, 1H), 7.38 (d, J = 8.1 Hz, 1H), 7.23 (t, J = 7.5 Hz, 1H), 7.17 (t, J = 7.4 Hz, 1H), 7.00 (s, 1H), 2.38 (s, 3H). ^{13}C NMR (150 MHz, CHLOROFORM-D) δ (ppm) 136.3, 128.3, 121.9, 121.6, 119.1, 118.8, 111.8, 111.0, 9.7.



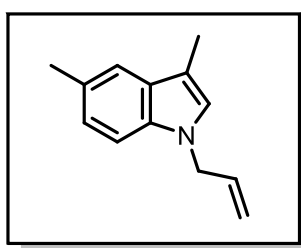
18. 10b, 3, 5-dimethyl-1H-indole, white crystalline solid: ^1H NMR (600 MHz, CHLOROFORM-D) δ (ppm) 7.79 (s, 1H), 7.42 (s, 1H), 7.27 (d, J = 8.2 Hz, 1H), 7.07 (d, J = 8.2 Hz, 1H), 6.96 (s, 1H), 2.52 (s, 3H), 2.36 (s, 3H). ^{13}C NMR (150 MHz, CHLOROFORM-D) δ (ppm) 134.6, 128.5, 128.3, 123.5, 121.8, 118.5, 111.2, 110.6, 21.5, 9.7.



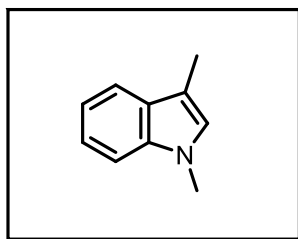
19. 10c, 3, 6-dimethyl-1H-indole, white crystalline solid: ^1H NMR (600 MHz CHLOROFORM-D) δ (ppm) 7.78 (s, 1H), 7.49 (d, $J = 7.9$ Hz, 1H), 7.29 (s, 1H), 6.98 (d, $J = 7.9$ Hz, 1H), 6.92 (s, 1H), 2.49 (s, 3H), 2.34 (s, 3H). ^{13}C NMR (150 MHz, CHLOROFORM-D) δ (ppm) 136.7, 131.6, 126.2, 120.9, 118.5, 111.6, 110.9, 21.7, 9.7.



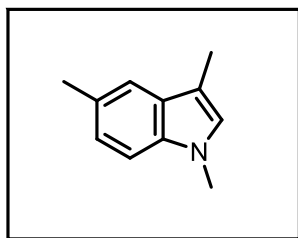
20. 10d, N-allyl-3-methyl-1H-indole, colourless oil: ^1H NMR (600 MHz CHLOROFORM-D) δ (ppm) 7.63 (d, $J = 7.9$ Hz, 1H), 7.33 (d, $J = 8.2$ Hz, 1H), 7.25 (t, $J = 7.6$ Hz, 1H), 7.16 (t, $J = 7.4$ Hz, 1H), 6.92 (s, 1H), 6.02 (ddd, $J = 16.1, 10.5, 5.2$ Hz, 1H), 5.18 (dd, $J = 51.4, 13.6$ Hz, 2H), 4.71 (d, $J = 5.3$ Hz, 2H), 2.38 (s, 3H). ^{13}C NMR (150 MHz, CHLOROFORM-D) δ 136.4, 133.8, 128.9, 125.5, 121.5, 119.0, 118.7, 117.0, 110.6, 109.4, 48.6, 9.6.



21. 10e, N-Allyl-3,5-dimethyl-1H-indole, colourless oil: ^1H NMR (600 MHz CHLOROFORM-D) δ (ppm) 7.41 (s, 1H), 7.21 (d, $J = 8.3$ Hz, 1H), 7.07 (d, $J = 8.3$ Hz, 1H), 6.87 (s, 1H), 6.01 (ddd, $J = 22.2, 10.5, 5.4$ Hz, 1H), 5.21 (d, $J = 10.2$ Hz, 1H), 5.12 (d, $J = 17.1$ Hz, 1H), 4.68 (d, $J = 5.2$ Hz, 2H), 2.52 (s, 3H), 2.35 (s, 3H). ^{13}C NMR (150 MHz, CHLOROFORM-D) δ 134.8, 134.0, 129.1, 127.9, 125.6, 123.0, 118.7, 116.9, 110.0, 109.1, 48.6, 21.5, 9.6.

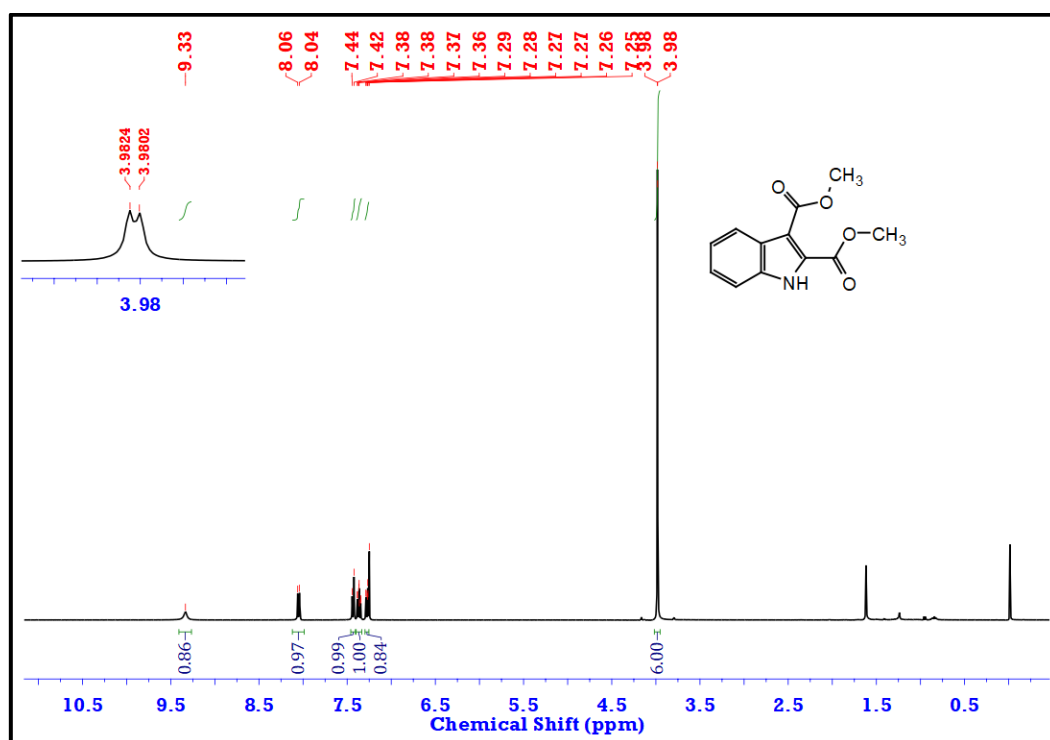
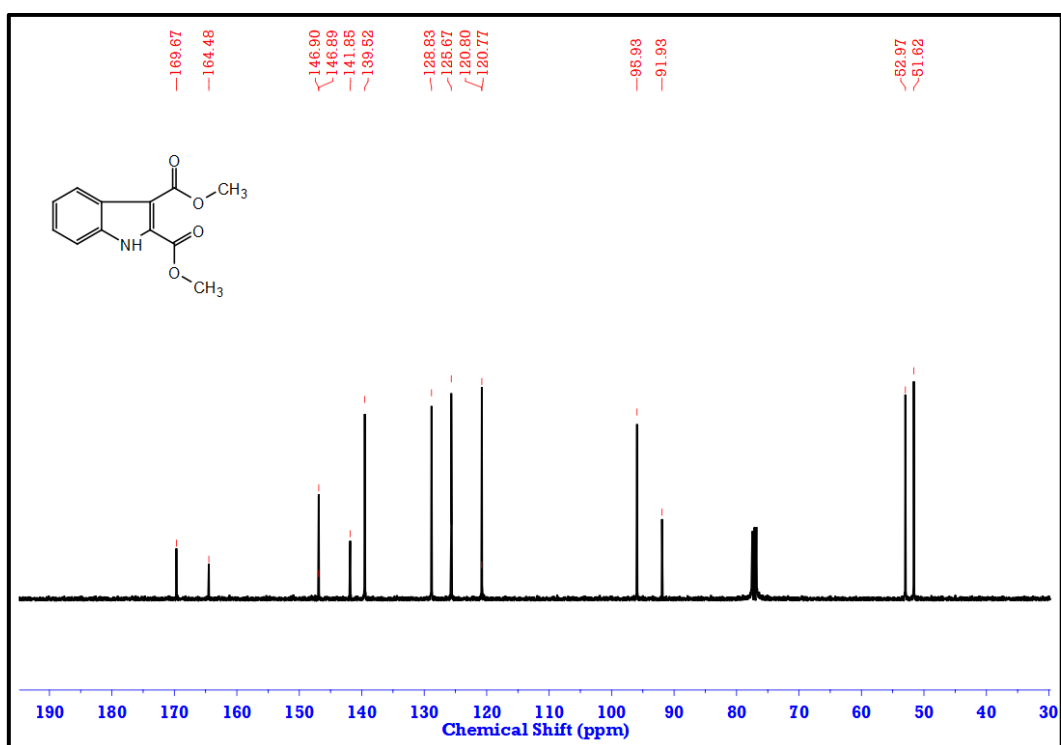


22. 10f, *N*-methyl-3-methyl-1*H*-indole, colourless oil: ^1H NMR (600 MHz CHLOROFORM- D) δ (ppm) 7.63 (d, $J = 7.9$ Hz, 1H), 7.33 (d, $J = 8.2$ Hz, 1H), 7.28 (d, $J = 7.6$ Hz, 1H), 7.16 (t, $J = 7.4$ Hz, 1H), 6.87 (s, 1H), 3.78 (s, 3H), 2.38 (s, 3H). ^{13}C NMR (150 MHz, CHLOROFORM- D) δ 137.0, 128.6, 126.5, 121.4, 118.9, 118.5, 110.1, 109.0, 32.5, 9.6.



23. 10g, 1,3,5-Trimethyl-1*H*-indole, colourless oil: ^1H NMR (600 MHz CHLOROFORM- D) δ (ppm) 7.40 (s, 1H), 7.22 (d, $J = 8.3$ Hz, 1H), 7.10 (d, $J = 8.2$ Hz, 1H), 6.82 (s, 1H), 3.75 (s, 3H), 2.53 (s, 3H), 2.35 (s, 3H). ^{13}C NMR (150 MHz, CHLOROFORM- D) δ (ppm) 135.5, 128.8, 127.7, 126.6, 123.0, 118.6, 109.5, 108.7, 32.5, 21.5, 9.6.

4.14. Representative NMR Spectra

Figure 4.6. ^1H NMR Spectrum of 9a (Dimethyl 1*H*-indole-2,3-dicarboxylate) in CDCl_3 Figure 4.7. ^{13}C NMR Spectrum of 9a (Dimethyl 1*H*-indole-2,3-dicarboxylate) in CDCl_3

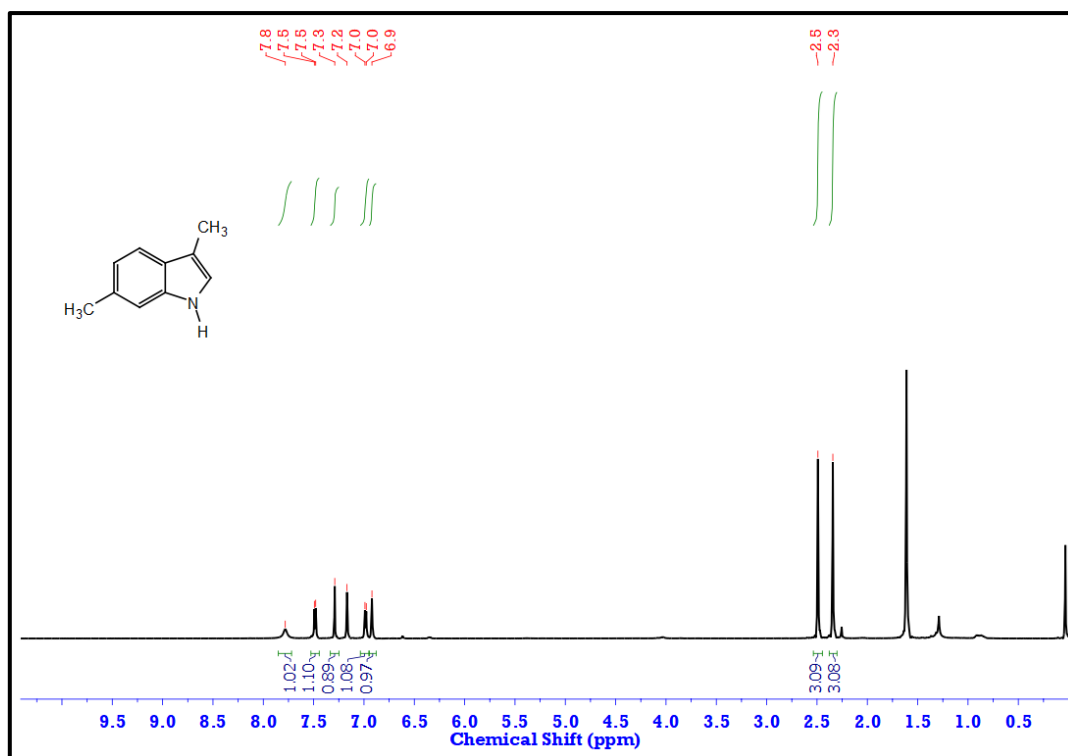


Figure 4.8. ^1H NMR Spectrum of 10c (3, 6-Dimethyl-1H-indole) in CDCl_3

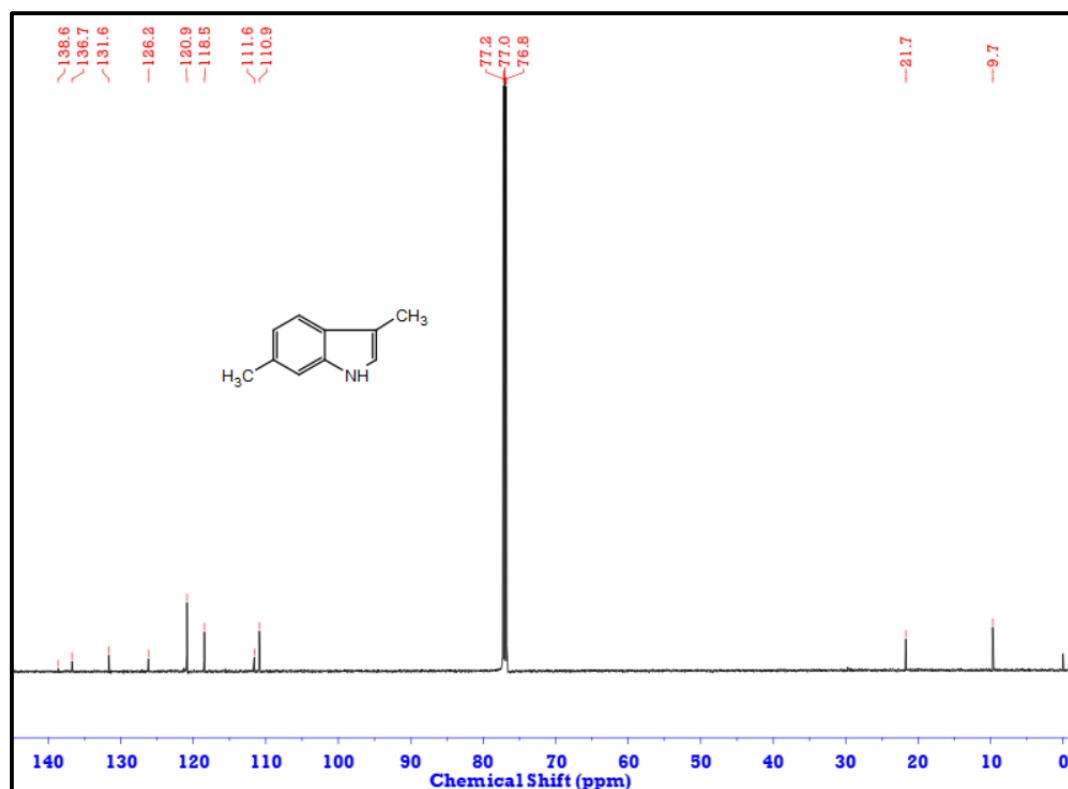


Figure 4.9. ^{13}C NMR Spectrum of 10c (3, 6-Dimethyl-1H-indole) in CDCl_3

4.15. Bibliography

- [1] a) Corbet, J. P. and Mignani, G. Selected patented cross-coupling reaction technologies. *Chemical Reviews*, 106(7):2651-2710, 2006; b) Suzuki, A. Recent advances in the cross-coupling reactions of organoboron derivatives with organic electrophiles. *Journal of Organometallic Chemistry*, 576(1-2):147-168, 1999; c) Ruiz-Castillo, P. and Buchwald, S. L. Applications of palladium-catalysed C–N cross-coupling reactions. *Chemical Reviews*, 116(19):12564-12649, 2016.
- [2] Gnad, C., Abram, A., Urstöger, A., Weigl, F., Schuster, M. and Köhler, K. Leaching mechanism of different palladium surface species in Heck reactions of aryl bromides and chlorides. *ACS Catalysis*, 10(11):6030-6041, 2020.
- [3] Link, J. T. The intramolecular Heck reaction. *Organic Reactions*, 60:157-561, 2004.
- [4] a) Robinson, B. Studies on the Fischer indole synthesis. *Chemical Reviews*, 69(2):227-250, 1969; b) Gribble, G.W., 2000. Recent developments in indole ring synthesis—methodology and applications. *Journal of the Chemical Society, Perkin Transactions 1*, (7), pp.1045-1075; c) Bugaenko, D. I., Karchava, A. V. and Yurovskaya, M. A. Synthesis of indoles: recent advances. *Russian Chemical Reviews*, 88(2):99, 2019; d) Heravi, M. M., Rohani, S., Zadsirjan, V. and Zahedi, N. Fischer indole synthesis applied to the total synthesis of natural products. *RSC Advances*, 7(83):52852-52887, 2017.
- [5] Bartoli, G., Dalpozzo, R. and Nardi, M. Applications of Bartoli indole synthesis. *Chemical Society Reviews*, 43(13):4728-4750, 2014.
- [6] Patil, S. A., Patil, R. and Miller, D. D. Microwave-assisted synthesis of medicinally relevant indoles. *Current medicinal chemistry*, 18(4):615-637, 2011.
- [7] Dumitrascu, F. and Ilies, M. A. Recent advances in the Nenitzescu indole synthesis (1990–2019). *Advances in Heterocyclic Chemistry*, 133:65-157, 2021.
- [8] Wagaw, S., Yang, B. H. and Buchwald, S. L. A palladium-catalysed method for the preparation of indoles via the Fischer indole synthesis. *Journal of the American Chemical Society*, 121(44):10251-10263, 1999.

- [9] Larock, R. C. and Yum, E. K. Synthesis of indoles *via* palladium-catalysed heteroannulation of internal alkynes. *Journal of the American Chemical Society*, 113(17):6689-6690, 1991.
- [10] Chen, C. Y., Lieberman, D. R., Larsen, R. D., Verhoeven, T. R. and Reider, P. J. Syntheses of indoles *via* a palladium-catalysed annulation between iodoanilines and ketones. *The Journal of Organic Chemistry*, 62(9):2676-2677, 1997.
- [11] Jensen, T., Pedersen, H., Bang-Andersen, B., Madsen, R. and Jørgensen, M. Palladium-Catalysed Aryl Amination–Heck Cyclisation Cascade: A One-Flask Approach to 3-Substituted Indoles. *Angewandte Chemie International Edition*, 47(5):888-890, 2008.
- [12] a) Taber, D. F. and Tirunahari, P. K. Indole synthesis: a review and proposed classification. *Tetrahedron*, 67(38):7195-7210, 2011; b) Goswami, K., Chakraborty, A., Sinha, S. and Jana, A. Recent Advances in the Palladium-Catalysed Synthesis of Unnatural Tryptophans. *European Journal of Organic Chemistry*, 27(5):e202301028, 2024.
- [13] Odle, R., Blevins, B., Ratcliff, M. and Hegedus, L. S. Conversion of 2-halo-N-allylanilines to indoles *via* palladium (0) oxidative addition-insertion reactions. *The Journal of Organic Chemistry*, 45(13):2709-2710, 1980.
- [14] Larock, R. C. and Babu, S. Synthesis of nitrogen heterocycles *via* palladium-catalysed intramolecular cyclisation. *Tetrahedron Letters*, 28(44):5291-5294, 1987.
- [15] Li, J. J. Synthesis of novel 3-substituted pyrrolo [2, 3-*b*] quinoxalines *via* an intramolecular heck reaction on an aminoquinoxaline scaffold. *The Journal of Organic Chemistry*, 64(22):8425-8427, 1999.
- [16] Gelpke, A. E. S., Veerman, J. J., Goedheijt, M. S., Kamer, P. C., van Leeuwen, P. W. and Hiemstra, H. Synthesis and use of water-soluble sulfonated dibenzofuran-based phosphine ligands. *Tetrahedron*, 55(21):6657-6670, 1999.
- [17] Carroll, M. A. and Holmes, A. B. Palladium-catalysed carbon–carbon bond formation in supercritical carbon dioxide. *Chemical Communications*, 13:1395-1396, 1998.

- [18] Khan, F., Fatima, M., Shirzaei, M., Vo, Y., Amarasiri, M., Banwell, M. G., Ma, C., Ward, J. S. and Gardiner, M. G. Tandem Ullmann–Goldberg Cross-Coupling/Cyclopalladation-Reductive Elimination Reactions and Related Sequences Leading to Polyfunctionalised Benzofurans, Indoles, and Phthalanes. *Organic Letters*, 21(16):6342-6346, 2019.
- [19] Yang, H., Sun, P., Zhu, Y., Yan, H., Lu, L., Liu, D., Rong, G. and Mao, J. Palladium-catalysed synthesis of indoles *via* intramolecular Heck reaction. *Catalysis Communications*, 38:21-25, 2013.
- [20] For palladium nanomaterials in cross-coupling reactions: (a) Söğütlü, I., Mahmood, E. A., Shendy, S. A., Ebrahimiasl, S. and Vessally, E. Recent progress in application of nanocatalysts for carbonylative Suzuki cross-coupling reactions. *RSC Advances*, 11(4):2112-2125, 2021; (b) Hong, K., Sajjadi, M., Suh, J. M., Zhang, K., Nasrollahzadeh, M., Jang, H.W., Varma, R. S. and Shokouhimehr, M. Palladium nanoparticles on assorted nanostructured supports: applications for Suzuki, Heck, and Sonogashira cross-coupling reactions. *ACS Applied Nano Materials*, 3(3): 2070-2103, 2020; (c) Srivastava, A., Kaur, H., Pahuja, H., Rangarajan, T. M., Varma, R. S. and Pasricha, S. Optimal exploitation of supported heterogenized Pd nanoparticles for CC cross-coupling reactions. *Coordination Chemistry Reviews*, 507:215763, 2024; d) Ashraf, M., Ahmad, M. S., Inomata, Y., Ullah, N., Tahir, M. N. and Kida, T. Transition metal nanoparticles as nanocatalysts for Suzuki, Heck and Sonogashira cross-coupling reactions. *Coordination Chemistry Reviews*, 476:214928, 2023; (e) Mpungose, P. P., Vundla, Z. P., Maguire, G. E. and Friedrich, H. B. The current status of heterogeneous palladium catalysed Heck and Suzuki cross-coupling reactions. *Molecules*, 23(7):1676, 2018; (f) Ayogu, J. I. and Onoabedje, E. A. Prospects and Applications of Palladium Nanoparticles in the Cross-coupling of (hetero) aryl Halides and Related Analogues. *ChemistryOpen*, 10(4):430-450, 2021; (g) Shahzad, A., Saeed, H., Iqtedar, M., Hussain, S. Z., Kaleem, A., Abdullah, R., Sharif, S., Naz, S., Saleem, F., Aihetasham, A. and Chaudhary, A. Size-controlled production of silver nanoparticles by *Aspergillus fumigatus* BTCB10: likely antibacterial and cytotoxic effects. *Journal of Nanomaterials*, 2019(1):5168698, 2019; (j) Gholinejad, M., Naghshbandi, Z. and Nájera, C. Carbon-Derived Supports for Palladium Nanoparticles as Catalysts for Carbon-Carbon Bonds Formation. *ChemCatChem*, 11(7):1792-1823, 2019.

[21] a) Soni, J., Sahiba, N., Sethiya, A. and Agarwal, S. Polyethylene glycol: A promising approach for sustainable organic synthesis. *Journal of Molecular Liquids*, 315:113766, 2020; b) Divyavani, C., Padmaja, P. and Reddy, P. N. The Emerging Role of Polyethylene Glycol-water (PEG-H₂O) as the Benign Mixed Solvent System in Organic Synthesis. *Current Organic Synthesis*, 22(1):36-62, 2025; c) Gravert, D. J. and Janda, K. D. Organic synthesis on soluble polymer supports: liquid-phase methodologies. *Chemical Reviews*, 97(2):489-510, 1997; d) Serveshe, A., Lokesh Kumar, S., Govindaraju, S., Tabassum, S., Raj Prasad, J., Kumar, N. and Ramaraj, S. G., 2024. Recent advances in polyethylene glycol as a dual-functional agent in heterocycle synthesis: Solvent and catalyst. *Polymers for Advanced Technologies*, 35(6):e6433, 2024.

[21] Bruns, D. L., Musaev, D. G. and Stahl, S. S. Can donor ligands make Pd(OAc)₂ a stronger oxidant? access to elusive palladium (II) reduction potentials and effects of ancillary ligands *via* palladium (II)/hydroquinone redox equilibria. *Journal of the American Chemical Society*, 142(46):19678-19688, 2020.

[22] Negishi, E. I., Zhang, Y. and O'Connor, B. Efficient synthesis of carbobicyclic and carbopolycyclic compounds *via* intramolecular carbopalladation catalysed by palladium-phosphine complexes. *Tetrahedron Letters*, 29(24):2915-2918, 1988.

[23] Masters, J. J., Jung, D. K., Bornmann, W. G., Danishefsky, S. J. and de Gala, S. A concise synthesis of a highly functionalised C-aryl taxol analog by an intramolecular Heck olefination reaction. *Tetrahedron Letters*, 34(45):7253-7256, 1993.

[24] O'Connor, B., Zhang, Y., Negishi, E. I., Luo, F. T. and Cheng, J. W. Palladium-catalysed cyclisation of alkenyl and aryl halides containing α , β -unsaturated carbonyl groups *via* intramolecular carbopalladation. *Tetrahedron Letters*, 29(32):3903-3906, 1988.

[25] Ziegler, F. E., Chakraborty, U. R. and Weisenfeld, R. B. A palladium-catalysed carbon-carbon bond formation of conjugated dienones: A macrocyclic dienone lactone model for the carbomycins. *Tetrahedron*, 37(23):4035-4040, 1981.

[26] Negishi, E. I., Copéret, C., Ma, S., Liou, S. Y. and Liu, F. Cyclic carbopalladation. A versatile synthetic methodology for the construction of cyclic organic compounds. *Chemical Reviews*, 96(1):365-394, 1996.

[27] (a) Pei, X., Xiang, D., Luo, Z., Lei, F., Guo, Z., Liu, D., Zhao, Z., Ran, M. and Dai, T. Catalytic performance of palladium nanoparticles encapsulated within nitrogen-doped carbon during Heck reaction. *Journal of Catalysis*, 400:20-27, 2021; (b) Wang, Z., Xiao, P., Shen, B. and He, N. Synthesis of palladium-coated magnetic nanoparticle and its application in Heck reaction. *Colloids and Surfaces A: Physicochemical and Engineering Aspects*, 276(1-3):116-121, 2006.; (c) Trzeciak, A. M. and Ziółkowski, J. J. Monomolecular, nanosized and heterogenized palladium catalysts for the Heck reaction. *Coordination Chemistry Reviews*, 251(9-10):1281-1293, 2007; (d) Jin, T., Hicks, M., Kurdyla, D., Hrapovic, S., Lam, E. and Moores, A. Palladium nanoparticles supported on chitin-based nanomaterials as heterogeneous catalysts for the Heck coupling reaction. *Beilstein Journal of Organic Chemistry*, 16(1):2477-2483, 2020.; (e) Lan, Y., Ma, Y., Hou, Q., Luo, Z., Wang, L., Ran, M. and Dai, T. Immobilisation of palladium nanoparticles on polydopamine spheres with superior activity and reusability in Heck reaction. *Journal of Catalysis*, 430:115333, 2024; (f) Baran, N.Y., Baran, T. and Nasrollahzadeh, M. Synthesis of palladium nanoparticles stabilised on Schiff base-modified ZnO particles as a nanoscale catalyst for the phosphine-free Heck coupling reaction and 4-nitrophenol reduction. *Scientific Reports*, 13(1):12008, 2023; (g) Mirza-Aghayan, M., Mohammadi, M., Addad, A. and Boukherroub, R., 2020. Pd nanoparticles supported on reduced graphene oxide as an effective and reusable heterogeneous catalyst for the Mizoroki–Heck coupling reaction. *Applied Organometallic Chemistry*, 34(4):e5524, 2020.

[28] a) Dewan, A., Bharali, P., Bora, U. and Thakur, A. J. Starch assisted palladium (0) nanoparticles as *in-situ* generated catalysts for room temperature Suzuki–Miyaura reactions in water. *RSC Advances*, 6(14):11758-11762, 2016; b) Kusy, R. and Grela, K. Ligand-free (*Z*)-selective transfer semihydrogenation of alkynes catalysed by *in-situ* generated oxidizable copper nanoparticles. *Green Chemistry*, 23(15):5494-5502, 2021; c) Dong, Y., Chen, Y. Q., Jv, J. J., Li, Y., Li, W. H. and Dong, Y. B. Porous organic polymer with *in-situ* generated palladium nanoparticles as a phase-transfer catalyst for Sonogashira cross-coupling reaction in water. *RSC Advances*, 9(38):21671-21678, 2019; d) Karimi, B., Bigdeli, A., Safari, A. A., Khorasani, M., Vali, H. and Khodadadi Karimvand, S. Aerobic oxidation of alcohols catalysed by *in-situ* generated gold nanoparticles inside the channels of periodic mesoporous organosilica with ionic liquid framework. *ACS Combinatorial Science*, 22(2):70-79, 2020; e) Deka, P., Deka, R.

C. and Bharali, P. *In-situ* generated copper nanoparticle catalysed reduction of 4-nitrophenol. *New Journal of Chemistry*, 38(4):1789-1793, 2014.

[29] Sakamoto, T., Nagano, T., Kondo, Y. and Yamanaka, H. Condensed heteroaromatic ring systems; XVII: 1 palladium-catalysed cyclisation of β -(2-halophenyl) amino substituted α , β -unsaturated ketones and esters to 2, 3-disubstituted indoles. *Synthesis*, 1990(03):215-218, 1990.

[30] Heravi, M. M., Moradi, R. and Malmir, M. Recent advances in the application of the Heck reaction in the synthesis of heterocyclic compounds: An update. *Current Organic Chemistry*, 22(2):165-198, 2018.

[31] Crisp, G. T. Variations on a theme—recent developments on the mechanism of the Heck reaction and their implications for synthesis. *Chemical Society Reviews*, 27(6):427-436, 1998.

[32] Glockler, G. Carbon-halogen bond energies and bond distances. *The Journal of Physical Chemistry*, 63(6):828-832, 1959.

[33] Stephan, M., Panther, J., Wilbert, F., Ozog, P. and Müller, T. J. Heck Reactions of Acrolein or Enones and Aryl Bromides—Synthesis of 3-Aryl Propenals or Propenones and Consecutive Application in Multicomponent Pyrazole Syntheses. *European Journal of Organic Chemistry*, 2020(14):2086-2092, 2020.

[34] Grigg, R., Stevenson, P. and Worakun, T. Regiospecific formation of 1, 3-dienes by the palladium catalysed intra-and inter-molecular coupling of vinyl halides. *Tetrahedron*, 44(7):2049-2054, 1988.

[35] Gibson, S. E., Guillo, N., Middleton, R. J., Thuilliez, A. and Tozer, M. J. Synthesis of conformationally constrained phenylalanine analogues *via* 7-, 8-and 9-endo Heck cyclisations. *Journal of the Chemical Society, Perkin Transactions*, 1 (4):447-456, 1997.[36] Muratake, H., Abe, I. and Natsume, M. Total synthesis of an antitumor antibiotic,(\pm)-duocarmycin SA. *Tetrahedron Letters*, 35(16):2573-2576, 1994.

[37] Yadav, D., Sharma, S. K. and Menon, R. S. Regioselective synthesis of arylsulfonyl heterocycles from bromoallyl sulfones *via* intramolecular Heck coupling reaction. *Organic & Biomolecular Chemistry*, 18(36):7188-7192, 2020.

- [38] Chen, A., Zhao, K., Zhang, H., Gan, X., Lei, M., Hu, L. Synthesis of 8-oxoprotoberberines using acid-mediated cyclisation or the Heck reaction. *Monatshefte Fur Chemie*, 143(5):825-830, 2012.
- [39] Piou, T., Neuville, L., Zhu, J. Spirocyclisation by palladium-catalysed domino Heck-direct C-H arylation reactions: Synthesis of spirodihydroquinolin-2-ones. *Organic Letters*, 14(14):3760-3763, 2012.
- [40] Macor, J. E., Blank, D. H., Post, R. J. and Ryan, K. The synthesis of a conformationally restricted analog of the anti-migraine drug sumatriptan. *Tetrahedron Letters*, 33(52):8011-8014, 1992.
- [41] Shi, L., Narula, C. K., Mak, K. T., Kao, L., Xu, Y. and Heck, R. F. Palladium-catalysed cyclisations of bromodialkenyl ethers and amines. *The Journal of Organic Chemistry*, 48(22):3894-3900, 1983.
- [42] Luly, J. R. and Rapoport, H. Routes to mitomycins. An improved synthesis of 7-methoxymitosene using palladium catalysis. *The Journal of Organic Chemistry*, 49(9):1671-1672, 1984.